Title

T cells promote distinct transcriptional programs of cutaneous inflammatory disease in human skin structural cells

Authors

Hannah A. DeBerg[1], Mitch L. Fahning[2], James D. Schlenker[3], William P. Schmitt[3], Iris K. Gratz[2,4,5], Jeffrey S. Carlin[6,7], Daniel J. Campbell[2,8], Peter A. Morawski[2,#]

Affiliations

[1] Center for Systems Immunology, Benaroya Research Institute, Seattle, Washington, USA.

[2] Center for Fundamental Immunology, Benaroya Research Institute, Seattle, Washington, USA.

[3] Plastic and Reconstructive Surgery, Virginia Mason Medical Center, Seattle, Washington, USA.

[4] Department of Biosciences, University of Salzburg, Salzburg, Austria.

[5] EB House Austria, Department of Dermatology, University Hospital of the Paracelsus Medical University, Salzburg, Austria.

[6] Center for Translational Immunology, Benaroya Research Institute, Seattle, Washington, USA.

[7] Division of Rheumatology, Virginia Mason Medical Center, Seattle, Washington, USA.

[8] Department of Immunology, University of Washington School of Medicine, Seattle, Washington, USA.

[#] Corresponding Author – Address: 1201 9th Ave, Seattle, Washington 98101, USA; Phone: 1(206)287-1052; E-mail: pmorawski@benaroyaresearch.org

Conflict-of-interest statement

The authors have declared that no conflict of interest exists.

Abstract

T cells coordinate with structural cells in the skin to promote appropriate inflammatory responses and subsequent restoration of barrier integrity following insult. Gene expression studies cataloging human skin have defined transcriptionally distinct structural cell populations in healthy tissue and identified inflammatory disease-associated changes in epithelial keratinocytes and dermal fibroblasts. Cutaneous T lymphocyte activity is implicated in the development of inflammatory skin disease, but the mechanisms by which T cells promote disease-associated changes in the skin remain unclear. We show that subsets of circulating and skin-resident $CD4^+$ T cells promote distinct transcriptional outcomes in human keratinocytes and fibroblasts. Using these *in vitro* generated transcriptional signatures, we identify T cell-dependent gene modules associated with inflammatory skin diseases *in vivo*, such as a set of T_h17 cell-induced genes in keratinocytes that are enriched in the skin of patients with psoriasis and normalized in response to anti-IL-17 therapy. Interrogating clinical trial findings using *in vitro* generated structural cell gene networks enables investigation of the immune-dependent contribution to inflammatory skin disease and the heterogeneous patient response to biologic therapy.

Introduction

The skin is an immunologically active barrier tissue specialized to deal with a litany of stresses. It contains many immune and structural cell populations whose frequencies and transcriptional profiles are altered during inflammatory skin disease[1–6]. For example, in the epidermis, 11 distinct cell states were described in healthy skin by single cell RNA-seq and disease-associated changes in keratinocyte (KC) gene programs were found in individuals with psoriasis (Ps)[1]. Transcriptional diversity in the dermis is similarly evident and supported by single cell analyses detailing the gene programs of structural cells such as fibroblasts, pericytes, and endothelial cells[3–6]. One study described 10 distinct dermal fibroblast (Fib) clusters in healthy skin and monitored these in individuals with systemic sclerosis (scleroderma, SSc). A progressive loss of LGR5-expressing Fibs (Fib-LGR5), a dominant gene signature in healthy skin, corresponded with SSc severity[4]. Despite the practical advances made in defining the broad transcriptional diversity of skin structural cells, a conceptual framework on how the distinct gene states of skin are regulated during health and disease is lacking.

Functionally specialized skin T cells cooperate with cells of the epidermis and dermis to respond to chemical, biological, and physical stresses[7]. Skin T cells are important in the context of responses to pathogens, allergens, and tumors, in barrier maintenance and wound healing, and they drive disease pathogenesis in many autoimmune and inflammatory diseases. Healthy adult human skin has an average surface area of $1.8m^2$ and contains numerically more T cells than any other non-lymphoid tissue: an estimated 2×10^{10} T cells or ~6% of the total T cell mass in the body[8]. Most skin T cells express cutaneous lymphocyte antigen (CLA), an inducible carbohydrate modification of P-selecting glycoprotein ligand-1 (PSGL-1) and other cell surface glycoproteins[9,10]. CLA-expressing T cells in the blood are a skin-tropic population expressing markers of tissue homing – CCR4, CCR6, CCR8, CCR10 – and make up 5-15% of the circulating $CD4^+$ T cell

pool. As with conventional circulating $CD4^+$ T cells, CLA^+ skin-tropic cells in the blood can be subdivided into distinct T_h subsets using standard chemokine receptor identification strategies[11]. In addition to traditional T_h subsets, we previously identified $CD4^+CLA^+CD103^+$ T cells, a distinct population of skin resident-memory T cells (T_{RM}) that have the capacity to exit the tissue and form a stable population of migratory T_{RM} in the circulation of healthy individuals[12]. We showed that $CD4^+CLA^+CD103^{neg}$ and $CD103^+$ skin-resident T cells from healthy control donors are transcriptionally, functionally, and clonally distinct populations. Collectively, $CD4^+$ T cells of the skin include functionally specialized populations, though how they exert their influence on the structural cells of the epidermis and dermis to coordinate essential aspects of skin biology remains incompletely understood.

The contribution of T cells and their cytokines is essential to the development of inflammatory skin disease. Accumulation of T cells in lesional tissue and T cell cytokines in patient serum often serve as indicators of active disease, while GWAS have identified polymorphisms in cytokines and cytokine receptors that increase the risk of developing inflammatory skin disease[13–15]. Attempts to target cytokine signaling therapeutically in the skin date back four decades to the use of recombinant IFN in cutaneous T cell lymphoma patients[16]. More recently, IL-17 and IL-23 neutralizing therapies have had immense success at reversing skin pathology during Ps[17,18]. Many candidate therapeutics aimed at altering the abundance or activity of T cell subsets and cytokines are now being used or tested in patients with inflammatory and autoimmune diseases including Ps, atopic dermatitis (AD, eczema), alopecia areata, hidradenitis suppurativa, and SSc[19,20]. While clinical interventions targeting T cell activity during inflammatory skin disease are promising, it remains unclear to what extent functionally specialized cutaneous T cell populations instruct the structural cell gene programs of healthy and diseased skin.

In this study, we show that different subsets of circulating and skin-resident $CD4^+$ T cells promote transcriptionally distinct states in primary human epithelial KCs and dermal Fibs including the induction of gene programs involved in the inflammatory response, proliferation, barrier integrity, and wound repair. We use this knowledge of T cell-dependent effects to investigate gene expression changes occurring during different inflammatory skin diseases and following intervention in these patients using anti-cytokine therapies. These data inform how T cells promote the diverse gene states of skin structural cells, forming the basis for a method to monitor immune-dependent differences between healthy and inflamed tissues and predict patient responses to T cell-targeted therapeutic interventions.

Results

Functional characterization of circulating and skin-resident human T cell populations

To assess T cell functional capacity, we isolated 7 distinct blood or skin derived $CD4^+CLA^+$ T_h subsets (*Blood*: T_h1, T_h2, T_h17, T_h22, $CD103^+$; *Skin*: $CD103^{neg}$, $CD103^+$) from healthy controls as described previously[11,12,21] (**Figure 1a, 1b**). Sorted T cell populations were stimulated through the TCR and co-stimulatory receptors for 48 hours and the production of 13 common T cell cytokines was measured in culture supernatants (**Figure 1c**, **S1**). As expected, T_h cell signature cytokines were enriched: T_h1 (IFNγ), T_h2 (IL-4, IL-5, IL-13), T_h17 (IL-

17A, IL-17F), T_h22 (IL-22), CD103$^+$ (IL-13, IL-22). Relative to the blood-derived T cells, those isolated from healthy skin produced lower levels of most measured cytokines (**Figure 1c**). However, both blood- and skin-derived T cells produced comparably high levels of IL-9, a transient signature cytokine of recently activated CLA$^+$ T cells (**Figure S1**)[10]. Thus, CD4$^+$CLA$^+$ T cell populations were found in both blood and skin and

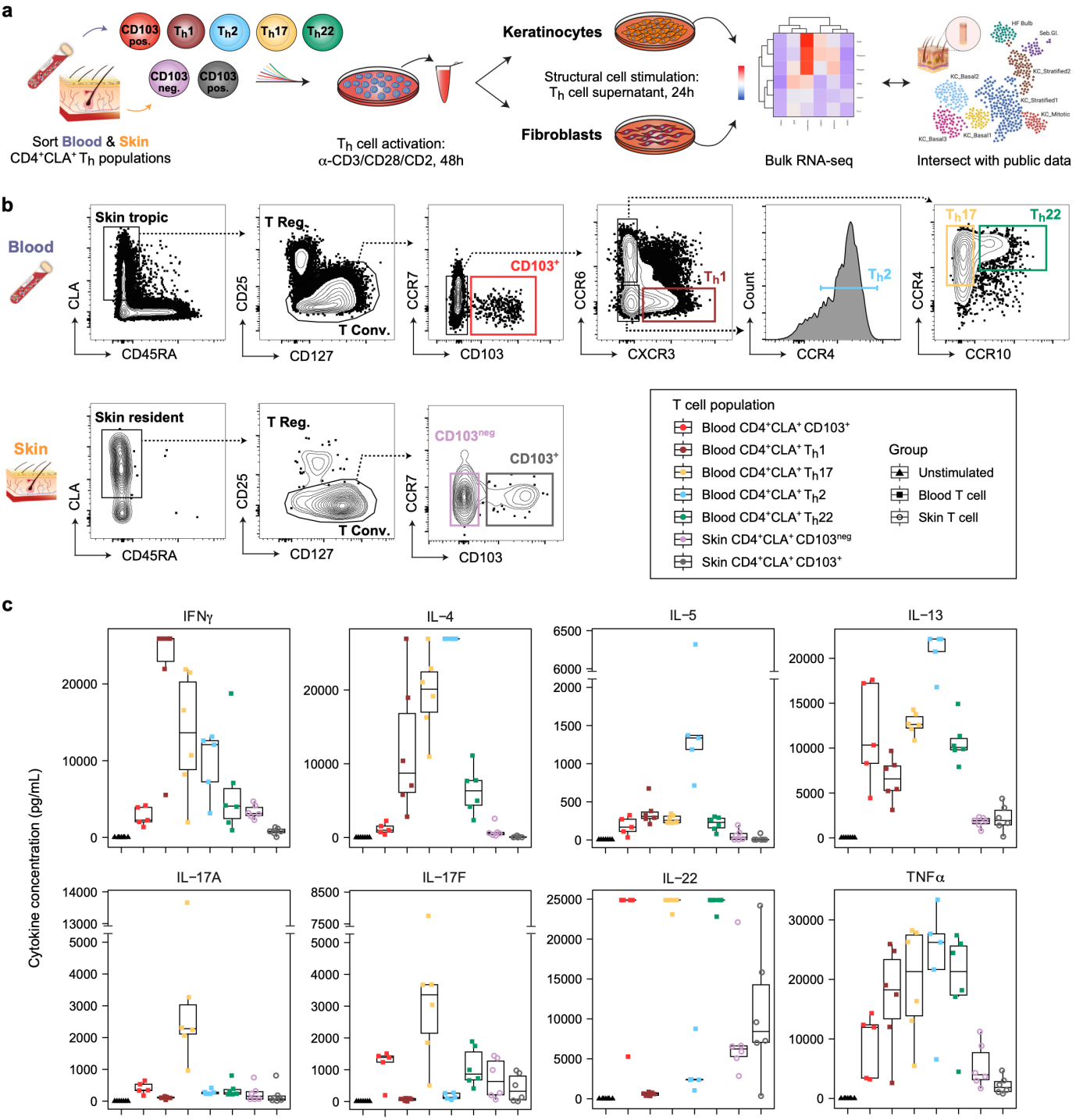

Figure 1. **Isolation and functional characterization of circulating and skin-resident human CD4$^+$CLA$^+$ T cell populations**. (**a**) Experimental design and study schematic: Blood and skin CD4$^+$CLA$^+$ T_h cell population isolation, activation, and subsequent stimulation of keratinocytes (KC) or fibroblasts (Fib), followed by structural cell gene expression analysis using bulk RNA-seq, and comparison to public gene expression data sets. (**b**) CD4$^+$CLA$^+$ T_h cell sorting strategy for indicated blood and skin cell populations. (T Conv, conventional T cells; T Reg, regulatory T cells). (**c**) Quantitative cytokine bead array measurement of all stimulated T cell supernatants for the 8 indicated analytes (n=5-6 donors per population). Full statistical analysis of cytokine production is provided in **Supplementary Table 1**.

produced signature cytokines that contribute to host defense, tissue repair, and have been implicated in many inflammatory skin diseases[22].

CD4$^+$CLA$^+$ T cells induce distinct transcriptional states in epithelial keratinocytes and dermal fibroblasts

Assessing the effects of individual cytokines on the skin has uncovered targeted aspects of tissue biology, but this approach fails to recreate the complexity of an inflammatory response. To determine how CD4$^+$CLA$^+$ T_h cell subsets impact the gene expression profiles of skin structural cells, we cultured T cell-stimulated supernatants from 5-7 distinct donors per sorted group together with healthy donor primary KCs or Fibs for 24 hours. Transcriptional changes were then assessed by bulk RNA-seq (**Figure 1a**). An unsupervised analysis using principal component analysis (PCA) revealed that the T cell tissue of origin and T_h cell population are the major sources of variance in the KC data (**Figure 2a, 2b**). Each CD4$^+$CLA$^+$ T cell population promoted a distinct transcriptional state in the KCs. The top differentially expressed (DE) genes in KCs across all conditions clustered according to both the T cell subset and its tissue of origin (**Figure 2c**). Patterns in T cell-induced gene expression were reflected by the concentrations of cytokines measured in the supernatant of those T cells (IFNγ, IL-4, IL-5, IL-13, IL-17A, IL17F, IL-22, TNFα). A subset of inflammatory response genes known to be induced by T_h1 (i.e. IDO1, CXCL11), T_h2 (i.e. CCL26, IL13RA2), and T_h17 cells (i.e. CSF3, IL23A) also showed expression patterns that corresponded with levels of IFNγ, IL-4/IL-5/IL-13, or IL-17A/F, respectively (**Figure 2d**). By comparison, skin derived CD103$^+$ T cells and to a lesser extent the migratory CD103$^+$ fraction from the blood drove the expression of genes associated with cell cycle and proliferation in KCs (i.e. MKI67, CDK1).

To understand the biological significance of T cell-dependent KC transcriptional states, we performed a functional enrichment analysis. Interferon response was largely T_h1 cell-dependent while IL-10 immunoregulatory signaling and chemokine receptor pathways were highly enriched in response to T_h17 cell supernatants (**Figure 2e, S2a-e**). Skin-derived T cell effects showed enrichment of keratinization and cell cycle pathway genes for CD103^{neg} and CD103$^+$ fractions, respectively (**Figure 2d, 2e, S2f, S2g**). T cell activity broadly altered the baseline cytokine response potential of epithelial cells, as evidenced by dramatic changes in cytokine receptor expression by KCs (**Figure S3**). At rest, KCs constitutively expressed genes required for responsiveness to most T cell cytokines we measured, although CSF2RA (GM-CSF receptor) expression was near the limit of detection and neither IL2RA nor IL5R was detected in either cell type. In response to stimulation, expression of IL10RB and IL22R1 were most highly induced in KCs and Fibs by T_h1 cells, corresponding to the level of IFNγ measured in stimulated cell supernatants. This is consistent with IFNγ induction of IL-10R as described in gut epithelial cells during barrier restoration[23]. IL17RA and IL17RC expression by KCs, required for IL-17 signaling, were strongly induced by most CD4$^+$CLA$^+$ T cells tested. Expression of IL2RG, the common gamma chain, was strongly induced in response to stimulation, which potentiates the response to multiple other cytokines (IL-2, IL-4, IL-7, IL-9, IL-15). Thus, the action of CD4$^+$CLA$^+$ T cell subsets is important in shaping the outcome of cutaneous immune responses.

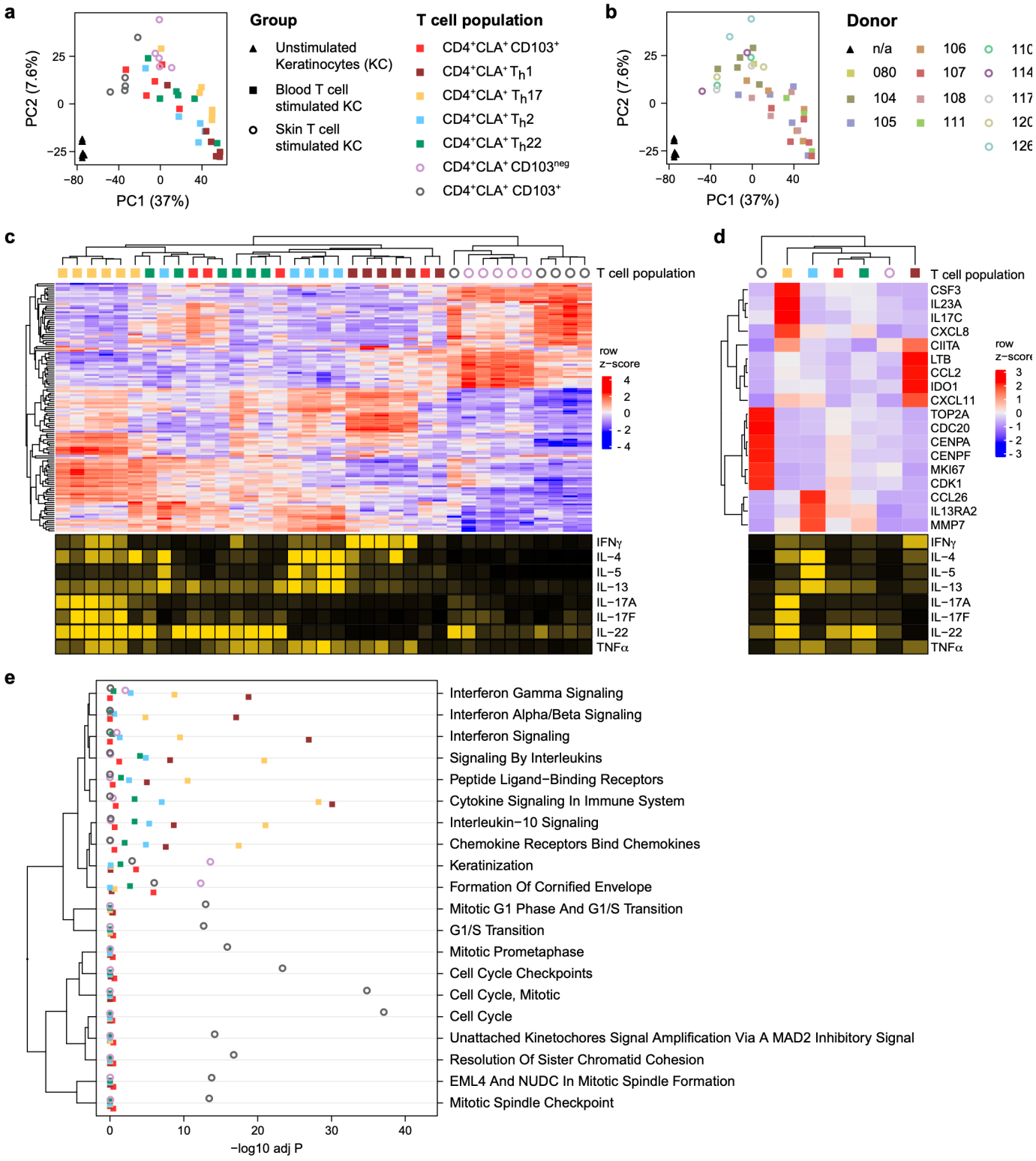

Figure 2. **CD4$^+$CLA$^+$ T cells induce distinct transcriptional states in epithelial keratinocytes**. (**a**) Principal component (PC) analysis of primary human KCs from a healthy donor cultured for 24 hours with the indicated activated blood- or skin-derived T cell supernatants, compared with matched unstimulated controls. (**b**) PC analysis showing each blood (n=7) and skin (n=5) healthy donor-treated KC sample. (**c,d**) *Top*: Heat map showing z-score expression changes of KC genes (*rows*) occurring in response to culture with the indicated donor T cell population supernatant (*columns*). *Bottom*: A relative measure of the cytokine production by each donor T cell population for indicated analytes, quantified in Figure 1. All measures are scaled by quantile with IL-5, IL-17a, and IL-17f which are truncated at the 95% quantile due to extreme outliers (c) The top 20 differentially expressed KC genes are shown in response to each indicated donor T cell population. (d) Expression of 18 well-characterized inflammatory and proliferative response elements in KC averaged across all donor samples for each indicated T cell subset. (**e**) Dot plot showing functional enrichment analysis of differentially expressed, T cell-induced KC genes within the indicated modules (n=5-6 donors per population). The -log10 adjusted P value is plotted as a statistical measure for enrichment within each module.

As observed with KCs, stimulation with blood and skin T cell supernatants had a strong effect on the dermal Fib gene programs in a healthy donor (**Figure 3a**). The largest effect size comes from T cell tissue of origin – blood versus skin – and while the impact of individual T_h populations was evident, this was less pronounced than that observed in KCs as seen both by PCA and DE gene analyses (**Figure 3a-c, S4**). The top DE genes in Fibs were separated into three main blocks: those associated with T_h1 activity and high levels of the pro-inflammatory cytokine IFNγ; those associated with blood-derived T_h cells producing either type 2 or type 17-associated cytokines; and those associated with skin-derived T cells that largely produced IL-22 and IL-9 (**Figure 3c**). Each T cell population induced a different set of genes, though the main response in Fibs occurs largely downstream of either T_h1/IFNγ or T_h17/IL-17 (**Figure 3d, S4b, S4c**). Fib cell cycle and proliferation genes were elevated in response to skin-derived T cell supernatants, as described in KCs, but also T_h17 and blood $CD103^+$ activity. Pathway analysis of the Fib response revealed broad engagement of cytokine signaling downstream of canonical $CD4^+$ T cell cytokines including IFNγ, IL-4, IL-13, and IL-10 (**Figure 3e**). Skin $CD103^{neg}$ T cells strongly promoted Fib responses to metal ions, an essential component of wound healing and the fibrotic response[24]. As with KCs, treatment with T cell supernatants substantially altered cytokine receptor expression on Fibs (**Figure S5**). For example, induction of IFNGR1 and IL17RA in Fibs was induced by both blood- and skin-derived $CD4^+CLA^+$ T cells, consistent with our observation that a large part of the dermal Fib response to T cells is dependent on T_h1/IFNγ and T_h17/IL-17 signaling. In contrast, IL13RA2 expression is promoted by T_h2, T_h17, T_h22 and blood $CD103^+$ T cells, which each produce varying degrees of IL-13 and low levels of IFNγ. Once thought to be only a decoy receptor, IL13RA2 is an important mediator of IL-13-dependent fibrotic responses in barrier tissues[25,26]. The baseline expression of IL31RA and OSMR were also elevated in stimulated Fibs, potentiating responsiveness to IL-31, a T cell cytokine involved in pruritis and atopic dermatitis[27,28]. Finally, TGFBR1 and TGFBR2 expression were antagonized by blood- but not skin-derived $CD4^+CLA^+$ T cells. Collectively, these data show that $CD4^+CLA^+$ T cells can induce transcriptionally distinct states in epithelial KCs and dermal Fibs including those associated with inflammatory, regulatory, proliferative, and fibrotic gene programs of the skin.

T cell-dependent gene signatures are enriched in the epidermis during inflammatory skin disease and normalized by anti-cytokine therapy

Phenotypically and functionally distinct T cell populations accumulate in lesional tissue during inflammatory and autoimmune skin diseases[7,13]. Ps (~3% prevalence in the US) and AD (~7% prevalence in the US) are two common skin inflammatory diseases in which dysregulated T cell responses are central to tissue pathology[7,29,30]. Ps is primarily associated with elevated T_h17 cell and IL-17 responses in the skin, whereas AD is driven largely by cutaneous T_h2 cells and IL-13 activity, while IL-4 and IL-5 responses are mostly absent[31,32]. The pathogenic role of T cell-derived cytokines in these diseases is highlighted by the success of biologic therapies: secukinumab and ixekizumab for Ps (anti-IL-17A); dupilumab and tralokinumab for AD (anti-IL4Rα, anti-IL13)[33–36]. Using the structural cell gene signatures generated in Figures 2 and 3, we assessed the relationships between T cell activity, dysfunctional gene programs in skin structural cells during

inflammatory disease, and patient responses to anti-cytokine therapy. As KCs are the majority population in the epidermis and alongside Fibs are the most abundant cells in human skin[37], we expected an analysis of full thickness skin biopsies would largely reflect changes in KC and Fib gene programs.

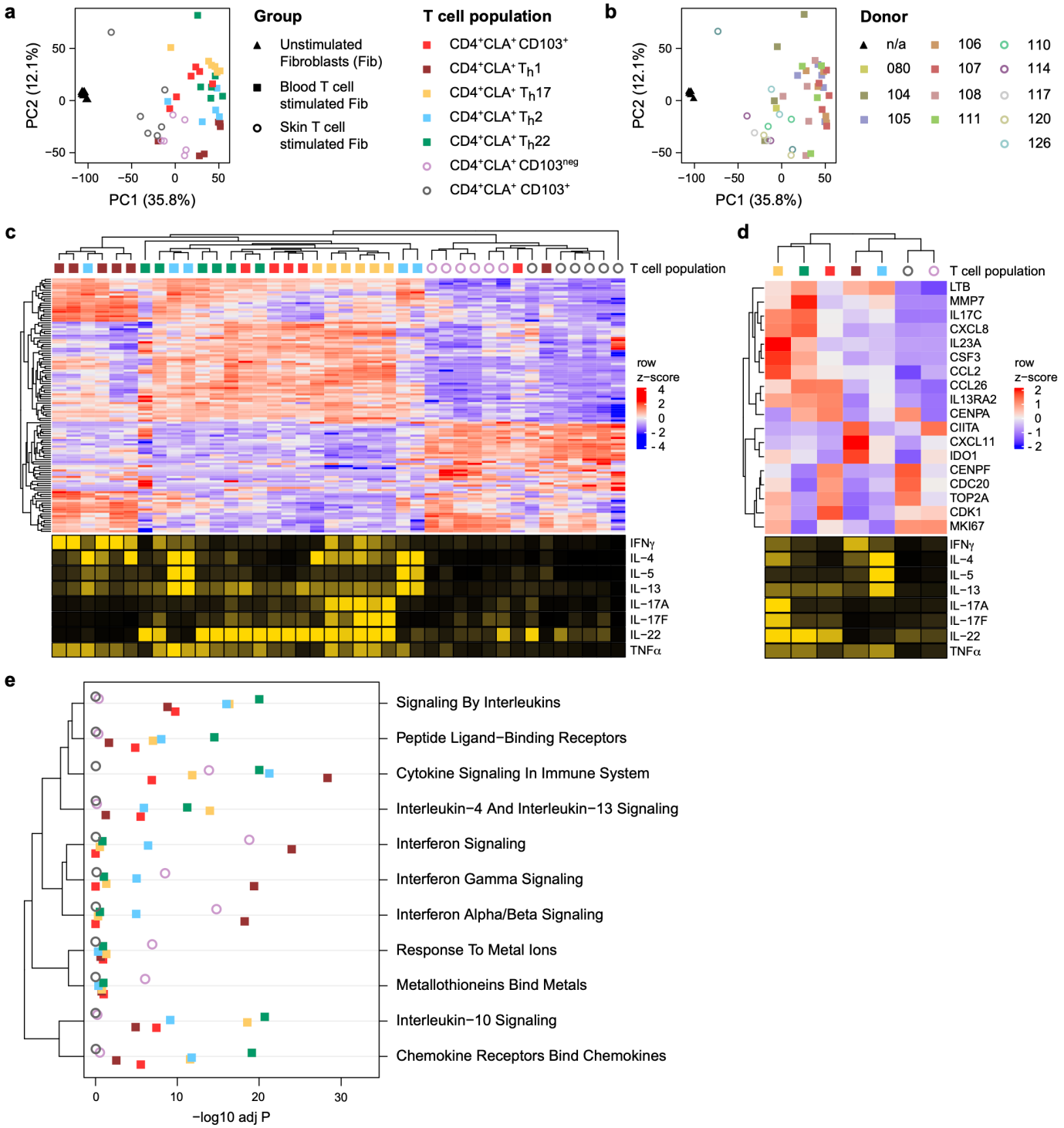

Figure 3. **CD4$^+$CLA$^+$ T cells induce distinct transcriptional states in dermal fibroblasts**. (**a**) Principal component (PC) analysis of primary human Fibs from a healthy donor cultured for 24 hours with the indicated activated blood- or skin-derived T cell supernatants, compared with matched unstimulated controls. (**b**) PC analysis showing each blood (n=7) and skin (n=5) healthy donor-treated Fib sample. (**c,d**) *Top*: Heat map showing z-score expression changes of Fib genes (*rows*) occurring in response to culture with the indicated donor T cell population supernatant (*columns*). *Bottom*: A relative measure of the cytokine production by each donor T cell population for indicated analytes, quantified in Figure 1. All measures are scaled by quantile with IL-5, IL-17a, and IL-17f which are truncated at the 95% quantile due to extreme outliers. (c) The top 20 differentially expressed Fib genes are shown in response to each indicated donor T cell population. (d) Expression of 18 well-characterized inflammatory and proliferative response elements in Fibs averaged across all donor samples for each indicated T cell subset. (**e**) Dot plot showing functional enrichment analysis of differentially expressed, T cell-induced Fib genes within the indicated modules (n=5-6 donors per population). The -log10 adjusted P value is plotted as a statistical measure for enrichment within each module.

We combined publicly available gene expression data of lesional, non-lesional, and healthy control donor skin from three clinical trials [GSE137218, GSE166388, GSE31652][38–40] that demonstrated the efficacy of anti-IL-17A therapies in patients with Ps, then applied batch correction to adjust for study-specific effects. The concatenated transcriptomic data sets clustered by disease state and treatment (**Figure 4a, S6a**). Differential gene expression analysis revealed a transcriptional profile shared across donor lesional skin samples before treatment initiation, and over the course of anti-cytokine therapy the transcriptome of Ps patient skin shifted to resemble that of healthy control and non-lesional skin (**Figure 4b**), reflecting the efficacy observed for these drugs[41].

We next looked for T cell-dependent gene expression changes in Ps patient skin over the course of anti-IL-17A therapy. We found that gene signatures induced by T cell populations in KCs (**Figure 2**) were broadly increased as a part of the dysregulated transcriptional signature of disease (**Figure 4c**). The T_h17-KC gene signature showed both the strongest association with the transcriptional dysregulation measured in Ps lesional skin and the response to therapy, compared to other T-dependent effects measured (**Figure 4d**). By day 84, both T_h17-KC and T_h22-KC signatures were decreased in patient skin in response to therapy relative to day 0 lesional skin, consistent with the known role of IL-17 producing $CD4^+$ T cells in Ps (**Figure 4c, 4d**). Of the 93 T_h17-induced signature genes measured in patient skin biopsies by microarray analysis (**Figure S2c**), we found 24 (26%) that were DE between Ps and healthy skin. Of these 24 genes, 13 (54%) were significantly responsive to anti-IL-17A therapy while 11 (46%) were not (**Figure S6b**). We assessed the expression changes of all T cell signature genes in Ps donor skin and found that many of the largest differences observed were for T_h17-induced genes, especially those that are both disease-associated and responsive to therapy (**Figure 4e**).

Further investigation revealed T_h17-dependent KC genes that have Ps-associated GWAS SNPs near their transcriptional start site (TSS) (**Figure 4f**). The risk allele *rs7556897* is located 10.3kb from the CCL20 gene[42]. It has a high variant-to-gene (V2G) score and impacts CCL20 as shown by expression and protein quantitative trait locus (eQTL, pQTL) mapping studies[43–45]. Another, *rs9889296*, is located 75.9kb from CCL8 and is implicated by fine mapping as an eQTL[42,46]. IL19 has 3 reported Ps GWAS hits: *rs3024493*, an eQTL for IL19 located 141bp from the TSS[42]; *rs55705316*, located 10.6kb from the TSS with Hi-C data showing promoter proximity[47,48]; *rs12075255*, 17.5kb from TSS[42]. CCL20 and CCL8 coordinate immune cell recruitment to the tissue[49] while IL19 is a part of the IL-17/IL-23 inflammatory axis of Ps and among the most DE cytokines measured between Ps[50]. Our analysis demonstrates that CCL20, CCL8, and IL19 are T_h17-dependent genes in KCs, which are each essential to the inflammatory axis in the epidermis of Ps patients and significantly impacted in those subjects undergoing anti-IL-17A therapy (**Figure 4f**). Published V2G mapping, eQTL and Hi-C studies complement our findings, reinforcing the functional relevance of these T cell-dependent target genes during Ps.

However, not all T-dependent KC genes that we identify as DE in lesional Ps skin were significantly impacted by anti-IL-17A therapy. Two examples are CXCL2, a neutrophil recruitment factor described to be

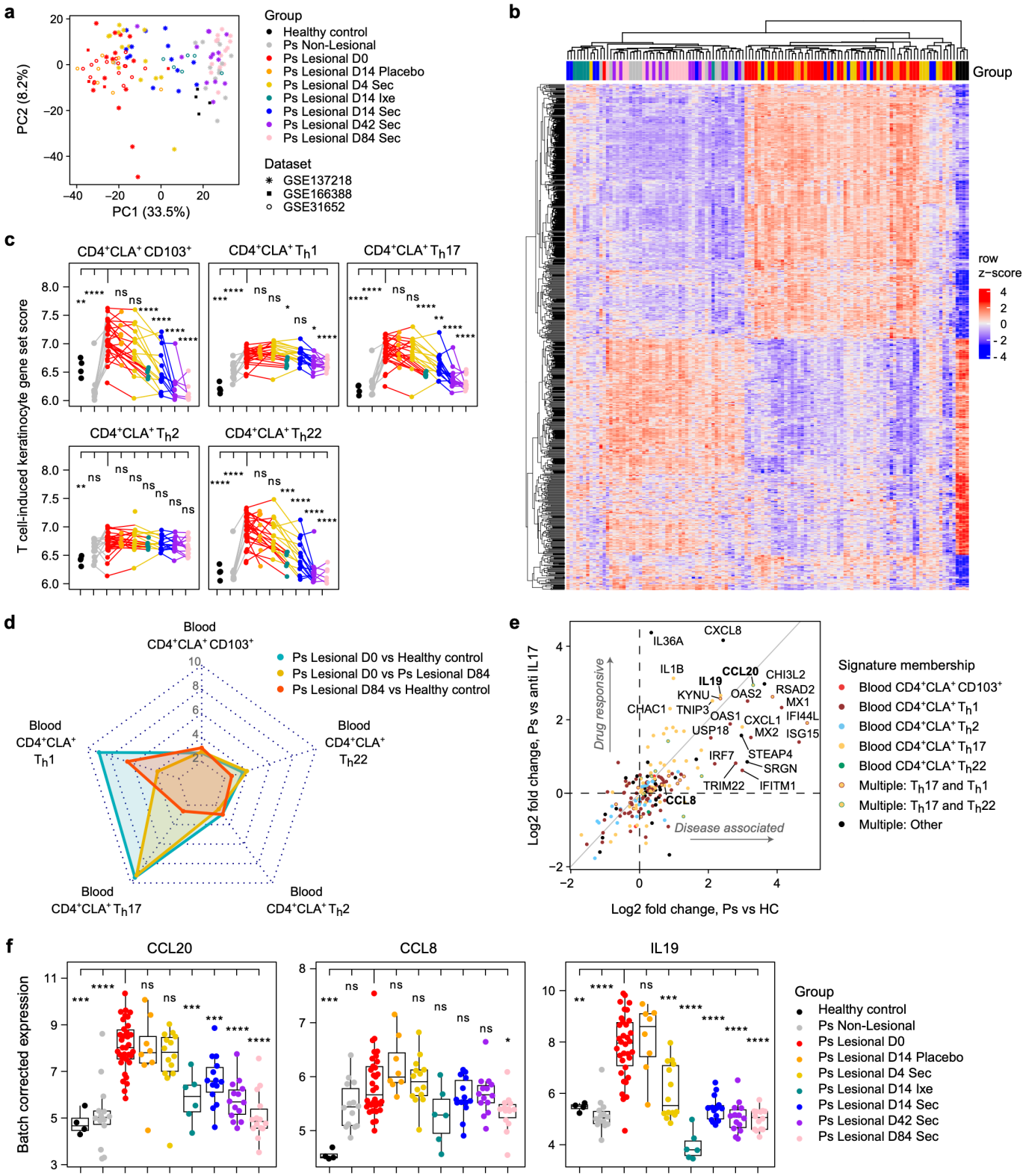

Figure 4. **T cell-dependent gene signatures are enriched in the epidermis during psoriasis and normalized by anti-IL-17A.** (**a**) PC analysis of gene expression in Ps lesional or non-lesional skin compared with healthy controls (HC) from the indicated public data sets. Ps patients were treated with an anti-IL-17A drug – secukinumab (Sec), ixekizumab (Ixe) – or placebo. Samples merged from these three data sets were batch corrected to adjust for study-specific effects. (**b**) Heat map showing z-score expression changes of KC genes determined to be T cell-dependent (Figure 2) within publicly available Ps patient data shown in 'a' for the indicated groups. (**c**) Plots show the gene set score analysis, an averaging of all T cell-dependent KC gene expression across all clinical trial subject groups. (**d**) Radar plots show T cell-KC signature gene enrichment values across the indicated pairwise comparisons from public clinical trial data (Ps and HC) with -log10 p-values increasing along the radial axis. (**e**) Bivariate plot of the log2 fold change between clinical trial subject groups for T cell-dependent KC genes (Ps vs HC, 'Disease associated'; Ps vs anti-IL17A, 'Drug responsive'). Individual genes are colored according to their T cell signature membership and compared genes altered in disease versus those responsive to therapy. (**f**) Plots show batch corrected gene expression for each clinical trial study group. Genes shown contain at least one known Ps GWAS-identified SNP and known to impact expression of that gene (i.e. eQTL). All statistical measures shown are compared to the Ps Lesional D0 group. Error bars indicate mean ± SD; ns = not significant, *p ≤ 0.05, **p ≤ 0.01, ***p ≤ 0.001, and ****p ≤ 0.0001 (Student's *t*-test).

part of the inflammatory axis of Ps[51], and NES, a gene encoding the intermediate filament nestin, which is expressed in skin epidermal stem cells and posited to be important during epithelial cell proliferation[52] (**Figure S6b**). CXCL2 and NES along with 9 other T_h17-dependent genes are Ps-associated, but their expression is not significantly altered by anti-IL-17A blockade. Thus, we report a variable effect of *in vivo* cytokine blockade on T cell-dependent gene expression in the skin, though it remains unclear which of these genes are central indicators of patient outcome to therapy.

We took a similar approach to analyze publicly available skin biopsy RNA-seq data from an AD clinical trial that tested the efficacy of IL-4R blockade, which interferes with both IL-4 and IL-13 cytokine activity [GSE157194][53], and from matched AD patients and controls [GSE121212][54]. Most of the variance in the combined data set could be explained by disease state, while a smaller effect was evident in response to treatment (**Figure 5a, S7a**). We focused our analysis on DE genes that we identified as T cell-dependent in KCs (**Figure 2**). Using this strategy, the data separated largely by lesional versus non-lesional and healthy skin. Samples in dupilumab treated groups were dispersed throughout hierarchical clusters, indicating a mild treatment effect on total T cell-dependent KC genes (**Figure 5b**). When comparing population-specific T cell-KC gene set expression across all patient groups we found a significant effect of dupilumab on the expression of $CD4^+CLA^+$ T_h2, T_h22, and $CD103^+$ T cell-dependent genes within lesional skin (**Figure 5c**). All T cell subset-KC gene sets were significantly upregulated within lesional skin compared with healthy skin, an effect that was diminished in response to therapy (**Figure 5c, 5d**). Dupilumab targets IL-4 and IL-13 activity, two cytokines made simultaneously and in abundance by $CD4^+CLA^+$ T_h2 cells (**Figure 1d**). We identified seven T_h2-induced KC genes that were both DE between lesional AD patient skin and controls and impacted by therapy (**Figure 5e, S7b**). Of these, CA2, SLC5A5, and SLC26A9 were significantly impacted by dupilumab in lesional AD patient skin (**Figure S7c**). CA2 encodes a carbonic anhydrase important for cellular pH and ion homeostasis, previously shown to be elevated in AD patient skin and differentiated KCs[55,56]. SLC5A5 and SLC26A9 encode iodine and chloride channel proteins, respectively, and neither have a known role in promoting pathology during AD. We now demonstrate that these 3 genes are directly T_h2-cell inducible in KCs and indicative of a positive patient outcome to dupilumab therapy.

Our findings demonstrate that T cell-dependent KC gene networks experimentally derived *in vitro* are: (1) enriched *in vivo* within human tissue; (2) associated with inflammatory skin disease; and (3) normalized in response to anti-cytokine biologic therapy. Further disease relevance is highlighted by fine-mapping studies that link GWAS-identified SNPs to the expression of T-dependent genes we describe. Thus, we validate a method of identifying candidate genes to explain immune-dependent effects during inflammatory disease and patient response to therapy. Importantly, some of the T-dependent KC genes we identify that are enriched in lesional patient skin *are not responsive* to FDA approved drugs assessed in this study, information that could be used to develop new therapeutic strategies targeting these gene networks in patients that fail to respond to a given biologic intervention.

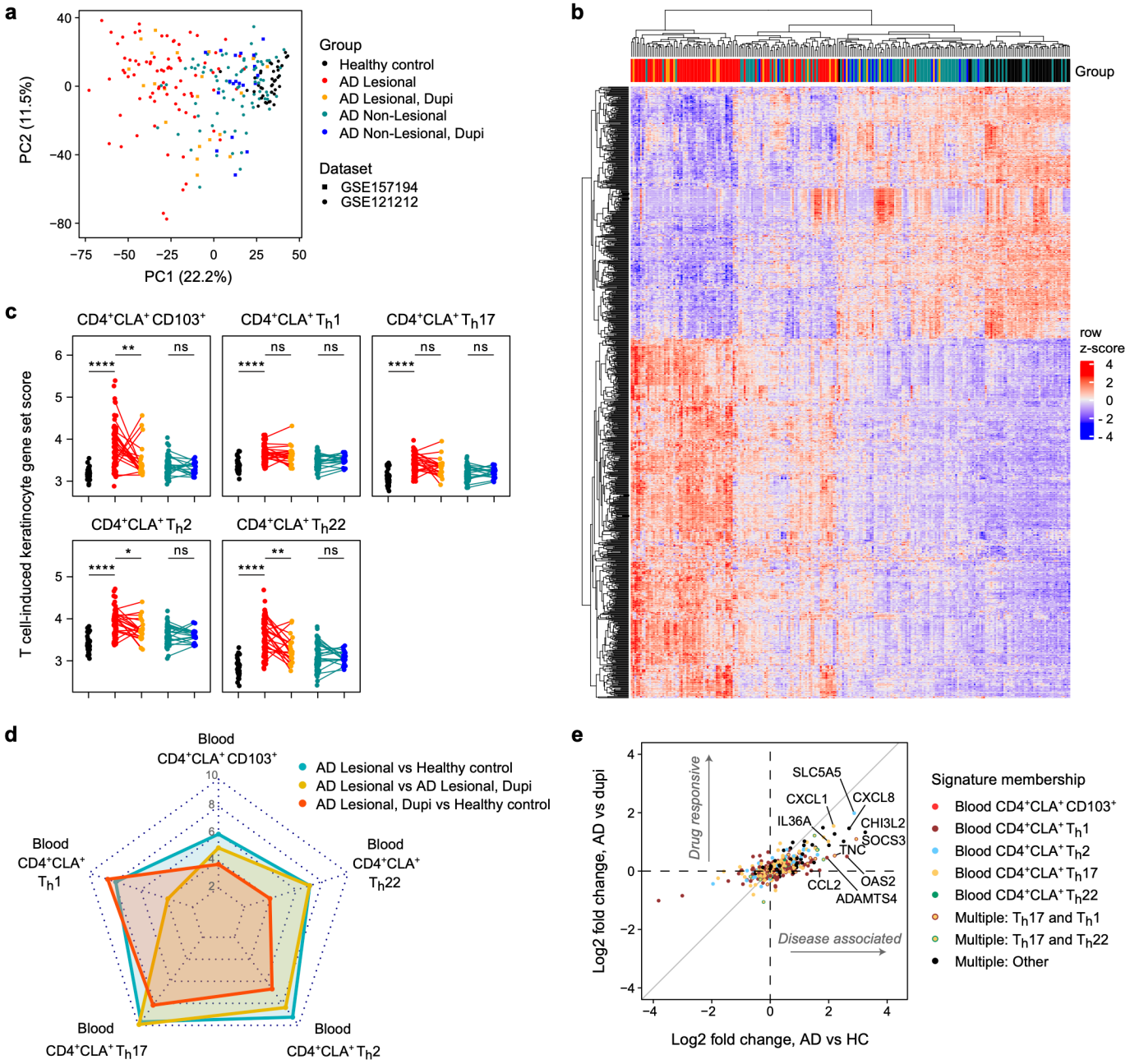

Figure 5. **T cell-dependent gene signatures are enriched in the epidermis during atopic dermatitis and normalized by anti-IL-4Rα therapy**. (**a**) PC analysis of gene expression data of AD donor lesional or non-lesional skin compared with healthy controls (HC) from the indicated publicly available data sets. AD patients were treated with dupilumab (Dupi), an anti-IL-4Rα drug. Samples merged from these two data sets were batch corrected to adjust for study-specific effects. (**b**) Heat map showing z-score expression changes of KC genes determined to be T cell-dependent (Figure 2) within publicly available AD patient data shown in 'a' for the indicated groups. (**c**) Plots show the gene set score analysis, an averaging of all T cell-dependent KC gene expression across all clinical trial subject groups. (**d**) Radar plots show T cell-KC signature gene enrichment values across the indicated pairwise comparisons from public clinical trial data (AD and HC) with -log10 p-values increasing along the radial axis. (**e**) Bivariate plot of the log2 fold change for T cell-dependent KC genes within public clinical trial data from AD or HC subjects (AD vs HC, 'Disease associated'; AD vs anti-IL17A, 'Drug responsive'). Individual genes are colored according to membership in a single or multiple T cell signature groups and compare genes altered in disease versus those responsive to therapy. Error bars indicate mean ± SD; ns = not significant, *p ≤ 0.05, **p ≤ 0.01, ***p ≤ 0.001, and ****p ≤ 0.0001 (Student's *t*-test).

T cell-dependent gene signatures are enriched in healthy skin fibroblast populations that are altered during fibrotic disease.

T cell infiltration and aberrant cytokine production can cause pathology such as tissue fibrosis and vascular abnormalities in people with fibrotic disease[57]. SSc is a rare inflammatory disease (~0.1% prevalence in the US) with highest mortality of any rheumatic illness. In the skin, pathology is commonly associated with

elevated T_h2 cell infiltration that promotes myofibroblast activity and alternatively activated macrophage differentiation[58,59]. Effective therapies for SSc are severely lacking and ongoing clinical trials are targeting T cell activation and cytokine signaling networks (i.e. IL-4, IL-13, TGFβ, IL-6, JAK/STAT)[60]. Despite strong evidence implicating T cells in fibrotic disease progression, the specific mechanisms by which T cells perturb stromal cell biology remain largely undefined.

To determine whether and to what extent T cell-dependent gene signatures can be found in dermal Fib populations and whether this changes during disease, we analyzed publicly available scRNA-seq data from SSc patients and healthy controls [GSE195452][4]. In this study, the authors identified 10 transcriptionally distinct Fib subsets including Fib-LGR5, a population that is selectively enriched in healthy skin and significantly diminished during severe SSc. The various functions of these Fib populations and their contribution to disease remain an area of intense interest. Our independent analysis of these data confirmed that LGR5 expression is enriched in healthy control Fibs compared with SSc donor cells (**Figure 6a, 6b**) and that the fraction of Fib-LGR5 is diminished progressively in patients with limited and diffuse cutaneous disease (**Figure 6c**). MYOC2 and POSTN Fib populations increased in the skin of SSc patients, corresponding with the decreased frequency of Fib-LGR5, elevated autoantibody levels, and increase in skin disease score (**Figure S8a, S8b**). T cell-dependent gene signatures (**Figure 3**) were detected throughout the 10 Fib subsets

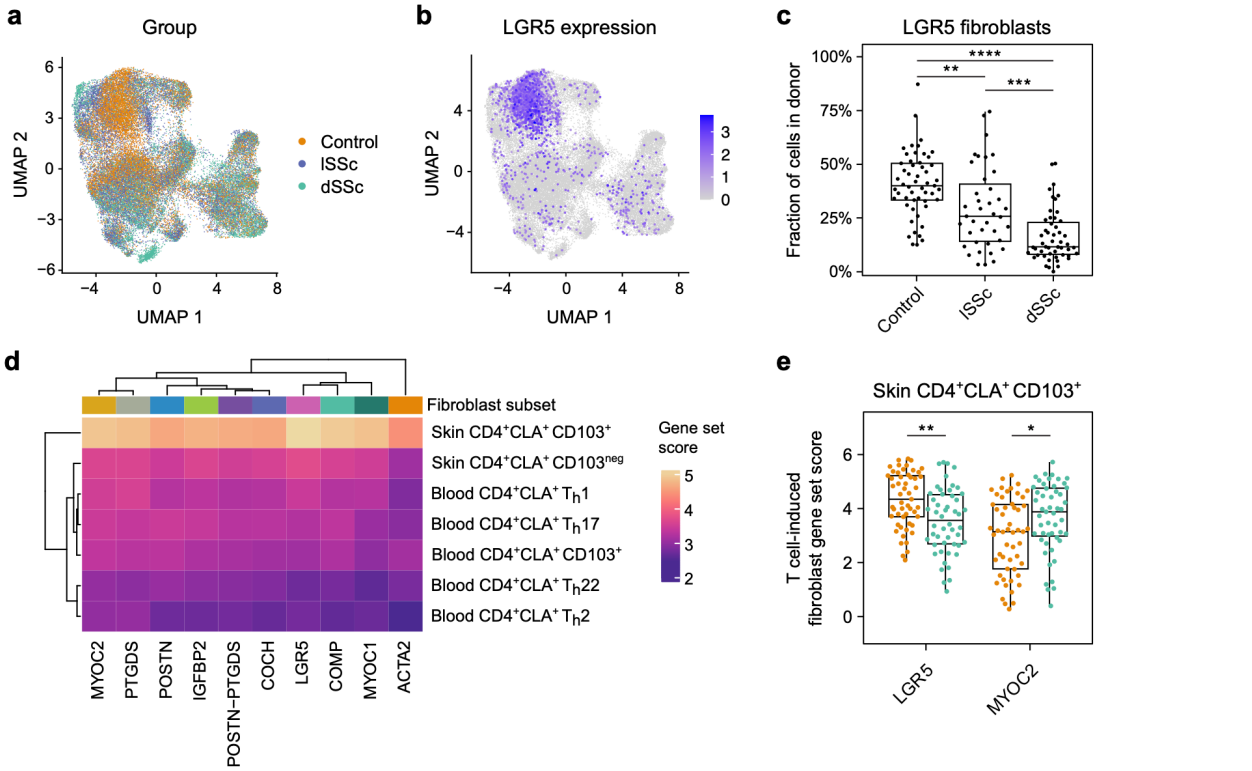

Figure 6. **T cell-dependent gene signatures are enriched in healthy donor dermal fibroblast populations that are altered during scleroderma**. Analysis of publicly available scRNA-seq data from donor skin biopsies [GSE195452]. (**a-c**) Uniform Manifold Approximation and Projection (UMAP) dimensionality reduction and cell frequency analysis of public RNA-seq data from full thickness skin biopsies, filtered to include only cells annotated as 'fibroblasts'. (a) Subject group information is overlaid onto UMAP space, including healthy controls and individuals with limited or diffuse systemic sclerosis (lSSc, dSSc). (b) Donor skin Fib log10 normalized expression of LGR5 plotted onto UMAP space. (c) Plot shows the frequency of the LGR5-Fib population as a percentage of total Fibs for each subject group. (**d**) Heat map shows the enrichment of T cell-dependent Fib gene signatures (Figure 3) within 10 described Fib subsets pseudobulk profiles from all three subject groups: Control, lSSc, dSSc. (**e**) Plot shows T cell-dependent gene signature enrichment score in LGR5-Fib and MYOC2-Fib of Control and dSSc profiles pseudobulked at the subject level. Error bars indicate mean ± SD; ns = not significant, *p ≤ 0.05, **p ≤ 0.01, ***p ≤ 0.001, and ****p ≤ 0.0001 (Student's *t*-test).

and the most pronounced effect observed was the enrichment of skin $CD4^+CD103^+$ T cell-induced genes in the Fib-LGR5 subset (**Figure 6d**). We also found that skin $CD4^+CD103^+$ T cell-dependent Fib gene enrichment observed in healthy donors Fib-LGR5 cells was reduced in severe SSc samples while the opposite effect was seen for the Fib-MYOC2 subset (**Figure 6e**). These data demonstrate that cutaneous $CD4^+$ T cells have the capacity to promote the gene programs of healthy skin-associated Fibs that are progressively diminished during fibrotic disease.

Discussion

In this study, we constructed an atlas of T cell-induced gene states in human skin, cataloging the transcriptional reprogramming of epidermal keratinocytes and dermal fibroblasts by $CD4^+CLA^+$ T_h cell populations and applying our findings towards an understanding of clinical data sets. Although the use of CLA to track cutaneous T cells goes back over two decades[9,10], our approach uniquely combines CLA identification of both blood- and skin-derived T cells together with chemokine receptor gating strategies and CD103 designation of migratory T_{RM}[11,12] to isolate broad and functionally diverse $CD4^+CLA^+$ T_h cells, which we leverage to study the changing transcriptional landscape of healthy and inflamed human skin.

T cells elicited significant effects on both KCs and Fibs, substantially altering the transcriptional landscape of both cell types. Cytokine-dependent gene modules were especially enriched, mainly through the activity of blood-derived CLA^+ T cells. There was abundant IFN-associated gene expression in both KCs and Fibs, most strongly induced by T_h1 cells in association with the highest levels of IFNγ. IL-4 and IL-13 responses were also highly engaged by blood-derived $CD4^+CLA^+$ T cell populations, but only in Fibs. Skin-derived T cells were more likely to promote gene networks required to execute critical homeostatic functions of skin. For example, keratinization, cornification, and proliferation processes – essential for maintenance and renewal of a healthy epithelium[61] – were induced specifically in KCs by $CD103^{neg}$ or $CD103^+$ skin T cells, while metal ion response pathways involved in wound healing[24] were induced by $CD103^{neg}$ T cells and only in Fibs. Thus, functionally unique $CD4^+CLA^+$ T cell populations promote distinct transcriptional outcomes in skin structural cells. These findings have important implications for how changes in T cell number and function in the skin impact the inflammatory response against harmful pathogens, but also the upkeep of homeostatic tissue functions such as barrier maintenance, recovery from injury, and regulated self-renewal.

Blocking T cell cytokine responses during Ps (IL-17) and AD (IL-4/IL-13) reduces leukocyte accumulation in the tissue and reverses skin pathology. While many studies have shown the efficacy of these drugs, not all patients meet the desired clinical endpoints and severe adverse events occur in a small but significant proportion of individuals, warranting further investigation to define the mechanisms of drug action and to identify new candidate drugs as alternative therapies[62–67]. Other drugs such as anti-TNFα or anti-IL-23 offer substitutes for Ps patients failing anti-IL-17A therapy, and the IL-13 specific agonist tralokinumab is an alternative for those with AD. Specific biomarkers of disease and the response to therapy will help guide the most effective course of treatment on an individual patient level. Our study adds important context that can help interpret clinical outcomes following anti-cytokine therapy. We describe the T cell-dependent gene

networks in KCs that are enriched in lesional skin of Ps and AD patients compared with non-lesional and healthy controls, and we demonstrate how the expression of these T-dependent genes is impacted during anti-cytokine therapy in patient skin.

By combining this approach with public immunogenetics data from Ps patients, we identified CCL20, CCL8, and IL19 as critical targets of anti-IL-17A therapy. Expression of each of these genes is elevated in lesional skin compared with controls, returned to baseline by therapy, and each contains GWAS risk alleles for Ps that are eQTL. Taken together with other published studies, our findings support a cooperative functional role for these genes: CCL20 recruits IL-17 producing $CCR6^+$ T_h17 cells to the skin that are implicated in Ps[49,68]; CCL8 can recruit many leukocytes including $CCR5^+$ $CD4^+$ T cells that are involved in barrier integrity maintenance and implicated in Ps pathogenesis[69,70]; IL-19 expression is positively associated with Psoriasis Area and Severity Index – a measure of skin pathology. Expression of IL-19 is both IL-17-dependent and further enhances the effects of IL-17A, increasing IL-23p19 expression and production of CCL20[50]. IL-19 is part of the IL-23/IL-17 inflammatory signaling network of Ps and is a proposed biomarker of disease. Guselkumab (anti-IL-23) is an approved drug for Ps that showed superior long-term efficacy to secukinumab[71], but no current therapy targets other components of the T cell/KC/Ps axis we describe such as IL-19, CCL8, or skin-tropic $CCR5^+$ T cells. Thus, the transcriptional network we describe in KCs is composed of individual genes known to potentiate a pro-inflammatory feed-forward loop in the epithelium, validating our approach for the identification of novel targets to monitor or manipulate during inflammatory skin disease.

We also assessed T cell-dependent effects on the epidermis and identified T_h2-dependent KC genes that are significantly altered in lesional AD patient skin, some of which were also responsive to dupilumab. For example, CA2 was previously shown to be induced in KCs and engineered skin equivalents by IL-4 and IL-13[56,72]. In comparison NTRK1, an early IL-13 target involved in allergic responses, is not clearly connected to AD[73]. Some of the genes we identify, such as TNC, CHI3L2 and SLC5A5, were shown to be upregulated in AD patient lesional skin[74–76], but in each case, the role of these factors in disease remain unclear. Thus, we describe an array of T cell-dependent targets in KCs, each representing a potentially new avenue of exploration to understand both the mechanisms of disease and responses to therapy in AD patients.

In the context of the dermis, our analyses revealed potential T cell-dependent Fib transcriptional networks including skin $CD4^+CD103^+$ T cell regulation of LGR5-Fib. The LGR5 expressing population is transcriptionally similar to PI16-Fibs described previously[3], with both LGR5- and PI16-Fibs independently shown to be reduced in SSc patient skin[4,77]. Individuals with severe SSc and reduced Fib-LGR5 are the most likely to have anti-topoisomerase I (scl-70) autoantibodies, which puts them at the highest risk for severe pulmonary fibrosis and end-organ disease[78]. Identifying immune-dependent events that support the survival or development of disease-associated Fib populations is therefore critical to devising new treatment strategies. We show that skin-resident $CD4^+CD103^+$ T cell-dependent genes are enriched in healthy donor LGR5-Fib compared with diffuse SSc patients. This raises the possibility that $CD4^+CD103^+$ T cell activity is essential to maintain LGR5-Fib in healthy skin, and that when perturbed during severe SSc, LGR5-Fib are lost and replaced by

myofibroblast lineages typical of fibrosis such as MYOC2-, SFRP2-, or PRSS23-Fib[6,79]. We have previously shown that skin CD103$^+$ T_{RM} cells uniquely co-produce IL-13 and IL-22 and have a TGFβ gene signature, implicating them in wound healing and barrier maintenance[12], but whether these T cells are altered in number or function within scleroderma patients remains unknown. We looked for T cell-dependent gene enrichment in Fibs from other published datasets[3,6,77] but found no statistically significant associations (*data not shown*). Thus, many open questions remain on the regulation of healthy skin- and SSc-associated Fibs by T cells, meriting further investigation to discern the critical immune-fibrotic axes of disease.

Our study design and subsequent analysis contains several caveats. First, we measure only 13 analytes produced by activated T cells, which accounts for only a fraction of the cytokines, metabolites and other soluble factors that are part of the T cell-dependent regulation of skin structural cell gene programs. Second, our study uses KCs and Fibs from a single anatomical skin site and so we are unable to comment on site-specific differences, for example owing to changes in moisture content, microbiome, or hair follicle density across this large barrier tissue. Finally, publicly available transcriptional data from interventional clinical trials that we assessed in this study were generated using either bulk sequencing or microarray methods. Future single-cell studies are required to solidify connections between a given T cell population or cytokine and specific gene networks within KC or Fib subsets during health and disease.

The atlas of T cell-dependent gene expression responses that we introduce in this study presents a new tool to facilitate a deeper understanding of the complex biology and transcriptional networks of skin. Through the practical application of our data to published clinical and human studies we were able to yield new insights into the pathogenesis of Ps, AD, and SSc. These observations reinforce the utility of our approach to dissect the immune-dependent contribution to inflammatory and fibrotic disease, and similar methodologies could be applied to understand the transcriptional response to pathogens or during barrier restoration following injury.

Methods

Human subject enrollment and study design

The objective of this research was to characterize the effect of human T cells on the gene expression profile of epithelial KCs and dermal Fibs. Immune cell isolation was performed using healthy blood and skin tissue – donor range 32 to 71 years of age. Human skin was obtained from patients undergoing elective surgery – panniculectomy or abdominoplasty. The cohort size was selected to ensure a greater than 80% probability of identifying an effect of >20% in measured variables. All samples were obtained upon written informed consent at Virginia Mason Franciscan Health (Seattle, WA). All study protocols were conducted according to Declaration of Helsinki principles and approved by the Institutional Review Board of Benaroya Research Institute (Seattle, WA).

Sex as a biological variable

Our study examined both male and female tissue with similar findings reported for both sexes. The study was not powered to detect sex-based differences.

Isolation of T cells from blood

PBMC were isolated using Ficoll-Hypaque (GE-Healthcare; GE17-1440-02) gradient separation. T cells were enriched using CD4 microbeads (Miltenyi; 130-045-101) then rested overnight at a concentration of 2 x 10^6 cells/mL in ImmunoCult™-XF T Cell Expansion Medium (StemCell; 10981) with 1% penicillin/streptomycin (Sigma-Aldrich; P0781) in a 15 cm^2 dish. The next morning cells were harvested and prepared for cell sorting, as indicated.

Isolation of T cells from skin

Fresh surgical discards of abdominal skin were treated with PBS + 0.1% Primocin (Invitrogen; ant-pm-1) for 5 minutes to eliminate contaminating microorganisms. Sterile tissue processing was performed on ice and skin was periodically sprayed with 1x PBS to keep samples from drying out. A biopsy tool (Integra™ Miltex™) was used to excise 4mm tissue biopsies from each sample. The subcutaneous fat was removed from biopsies before an overnight digestion of approximately 16 hours at 37°C, 5%CO_2. The digestion mix contained 0.8 mg/mL Collagenase Type 4 (Worthington; LS004186) and 0.04 mg/mL DNase (Sigma-Aldrich; DN25) in RPMI supplemented with 10% pooled male human serum (Sigma-Aldrich; H4522, lot SLC0690), 2 mM L-glutamine, 100 U/mL penicillin, and 100 mg/mL streptomycin. We used 1 mL of RPMI digestion media for each 40-50mg tissue in a 6-well non-tissue culture treated dish. The next morning tissue samples were washed excess RPMI + 3% FBS and combined into a single tube per donor. Filtration on a 100μM membrane was performed at each wash step, five total on average, to generate a single-cell suspension of skin mononuclear cells free of contaminating fat and debris. Skin mononuclear cell suspensions were then prepared for cell sorting, as indicated.

Flow cytometry, cell sorting, and fluorescently labeled antibodies

Cell labelling of surface antigens was performed with fluorescently tagged antibodies diluted in cell staining buffer containing HBSS and 0.3% BSA. A list of all antibody specificities, conjugated fluorophores, clones, vendors, catalog numbers, and final staining concentrations used to label blood- and skin-derived T cells is presented as a part of **Supplementary Table 5**. Viability dye staining using Fixable LiveDead was performed first in HBSS containing no additional protein, as recommended by the manufacturer. Surface staining was performed at 5% CO_2, 37°C for 20 minutes. Cell sorting of labelled samples was performed in cell sorting buffer – for yield sorts, HBSS + 5.0% BSA, for purity sorts HBSS + 1.0% BSA – using a BD FACSAria™ Fusion (85μM nozzle, 45 p.s.i.). The indicated conventional T_h cell populations (T_{Conv}) were sorted from blood and T_{Reg} were excluded by purity sort following $CD4^+$ T cell microbead enrichment. Skin mononuclear preparations were first enriched by a CD3 yield sort followed by purity sort of $CD4^+$ T_{Conv} and exclusion of T_{Reg}. Additional sample collection was performed using the BD LSR™ Fortessa cell analyzer. Resulting data (.FCS 3.1) were analyzed using FlowJo software (BD, v.10.9).

T cell stimulation and cytometric quantification of cytokines

Sorted T cell populations were pelleted by centrifugation at 300 x g for 5 minutes and resuspend in ImmunoCult™-XF T Cell Expansion Medium with 1% penicillin/streptomycin. Cultured T cells were stimulated for 48 hours at 1 x 10^6 cells/mL with ImmunoCult™ Human αCD3/αCD28/αCD2 T Cell Activator reagent (StemCell; 10970) used at the manufacturer recommended concentration. Cytokine containing supernatants from each unique donor were harvested and stored at -20C°. Frozen blood and skin activated T cell supernatants from all donors were thawed as a single batch to assess cytokine concentrations by cytometric bead array (BioLegend; LEGENDplex™ reagent) using a custom analyte panel: GM-CSF, IFNγ, IL-2, IL-4, IL-5, IL-6, IL-9, IL-10, IL-13, IL-17A, IL-17F, IL-22, TNFα. Data were analyzed using the manufacturer provided LEGENDplex software. The remaining thawed T cell supernatants were used immediately, without additional freeze-thaws, in culture of KCs or Fibs, as described. Freeze-thawed cell-free ImmunoCult™-XF T Cell Expansion Medium was used for unstimulated controls.

Keratinocyte and fibroblast cell culture and activation

Donor matched, primary human epithelial KCs and dermal Fibs were purchased from a commercial vendor (ZenBio; KR-F or DF-F) and cultured at low passages (p = 2-7) using either the KGM™ Keratinocyte Growth Medium BulletKit™ (Lonza; CC-3111) for KCs or DMEM supplemented with 10% FBS, 2 mM L-glutamine, 100 U/ml penicillin, and 100 mg/ml streptomycin (Gibco™; 10938025) for Fibs. Cytokine containing T cell supernatants were diluted using a 1:1 ratio of appropriate cell culture media and added to KCs or Fibs growing at 50% confluence – approximately 1-2 x 10^4 – in a 96-well flat bottom plate. Structural cells were cultured with activated T cell supernatants for 24 hours prior to isolation for RNA-sequencing (RNA-seq). Unstimulated controls used a 1:1 ratio of T cell media with either KC or Fib culture media.

Bulk RNA-sequencing (RNA-seq)

High-quality total RNA was isolated from approximately 2 x 10^4 T cell supernatant-treated KCs or Fibs using TRIzol™ Reagent (Invitrogen™; 15596026). Next, cDNA was prepared using the SMART-Seq v4 Ultra Low Input RNA Kit for Sequencing (Takara). Library construction was performed using the NexteraXT DNA sample preparation kit (Illumina) using half the recommended volumes and reagents. Dual-index, single-read sequencing of pooled libraries was run on a HiSeq2500 sequencer (Illumina) with 58-base reads and a target depth of 5 million reads per sample. Base-calling and demultiplexing were performed automatically on BaseSpace (Illumina) to generate FASTQ files.

Analysis of bulk RNA-seq data

The FASTQ files were processed to remove reads of zero length (fastq_trimmer v.1.0.0), remove adapter sequences (fastqmcf tool v.1.1.2), and perform quality trimming from both ends until a minimum base quality ≥ 30 (FASTQ quality trimmer tool v.1.0.0). Reads were aligned to the human reference genome (build hg38)

with TopHat (v.1.4.0) and read counts per Ensembl gene ID were quantified with htseq-count (v.0.4.1). Quality metrics for the FASTQ and BAM/SAM files were generated with FastQC (v.0.11.3) and Picard (v.1.128). Processing of FASTQ and BAM/SAM files was executed on the Galaxy workflow platform of Globus genomics. Statistical analysis of gene expression was assessed in the R environment (v.4.3.2). Sample inclusion for final analysis was based on a set of pre-established quality control criteria: total number of fastq reads > 1 x 10^6; mapped reads > 70%; median CV coverage < 0.85. Randomization was not applicable as no treatment or intervention groups were included in the study. Blinding was not applicable as no treatment groups were compared.

Additional bioinformatic analyses

All differential expression and pathway enrichment analyses were performed in R. To assess differential expression, the limma package (v.3.58.1) was used[80]. A log2 expression fold change of at least 1 in magnitude and an FDR of less than 0.05 were used as cutoffs to define differentially expressed genes. T cell-induced gene sets were formed by first excluding genes which were shared between all blood- or skin-cell-associated T cell-induced signatures and then selecting up to the top 200 differentially expressed genes ranked by FDR and associated with a T cell subset supernatant stimulation condition.

In analysis of public bulk microarray and RNA-seq GEO datasets, the ComBat function from the sva package (v.3.50.0) was used to adjust for dataset-specific batch effects[81]. Pathway enrichment analysis was performed using the enrichR package (v.3.2)[82] with the Reactome 2022 database[83] to query pathways associated with T cell-induced genes. T cell signatures were treated as a custom database and expression of these signatures were examined as lists of differentially expressed genes associated with Ps or AD.

GWAS hits associated with the trait “psoriasis” were downloaded from the NHGRI-EBI GWAS Catalog on February 7th, 2024. Within these results, GWAS SNPs with a “DISEASE/TRAIT” value of “Generalized pustular psoriasis”, “COVID-19 or psoriasis (trans-disease meta-analysis)”, or “Paradoxical eczema in biologic-treated plaque psoriasis” were excluded to ensure Ps-specific SNPs were analyzed[84].

Single cell gene expression data from SSc patient skin was re-analyzed using the Seurat R package (v.4)[85]. Pseudobulking was applied to defined Fib clusters [GSE195452][4] and the average expression of T cell-induced genes was computed for each pseudobulk profile as a gene set score.

Data availability

Values for all data points presented in figure graphs are reported in the **Supporting Data Values** file. All gene expression data sets generated in this study are available to the public in the Gene Expression Omnibus, **GSE272623**. Computer code generated and used for analysis in this study is available in Github:

- Commit URL, https://github.com/BenaroyaResearch/Morawski-T-cell-transcriptional-programs-in-skin
- Commit ID, 61c0224

Author Contributions

H.A.D., I.K.G., J.S.C., D.J.C. & P.A.M. designed research studies. J.D.S & W.P.S provided clinical samples. M.L.F & P.A.M. conducted wet bench experiments and acquired data. H.A.D. processed data and performed computational studies. H.A.D., D.J.C. & P.A.M. analyzed data and wrote the manuscript.

Acknowledgements

We are grateful to Kassidy Benoscek-Narag and the Clinical Research Center coordinators in the Benaroya Research Institute (BRI) Center for Interventional Immunology for human subject recruitment and sample collection, the BRI Genomics and Flow Cytometry facilities for technical assistance, and the BRI Scientific Writing Group for critical reading of the text. BRI cytometry and genomics equipment used in this study were generously supported by the M.J. Murdock Charitable Trust. This work was supported by a New Investigator research award (National Scleroderma Foundation) and R21AI185642 (NIAID, NIH) to P.A.M., R01AI127726 to I.K.G. and D.J.C. (NIAID, NIH), and R01AI177280 to H.A.D., I.K.G. and D.J.C. (NIAID, NIH).

Supplementary Figures

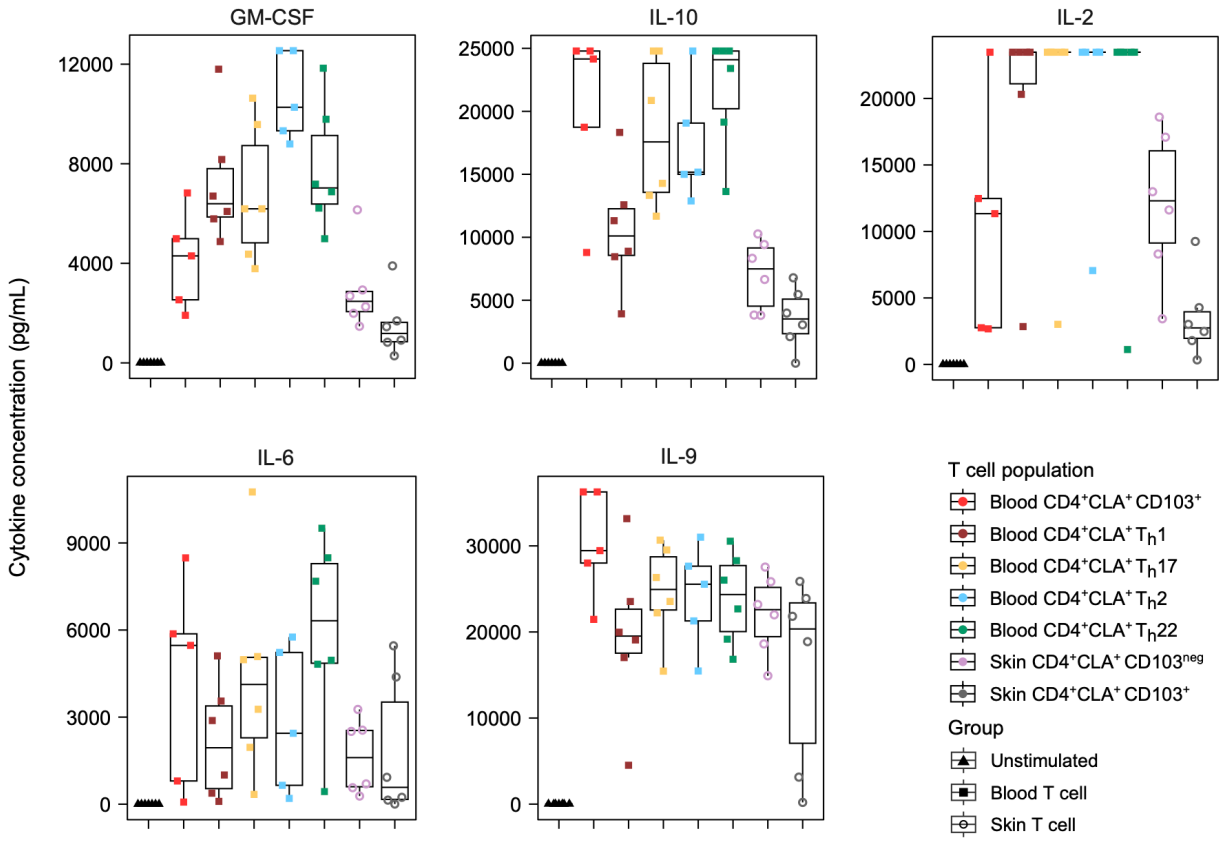

Supplementary Figure 1 (related to Figure 1). **Additional cytokine production capacity by circulating and skin-resident human CD4$^+$CLA$^+$ T cell populations**. Quantitative cytokine bead array measurement of all stimulated T cell supernatants for the 5 indicated analytes (n=5-6 donors per population). Full statistical analysis of cytokine production is provided in **Supplementary Table 1**.

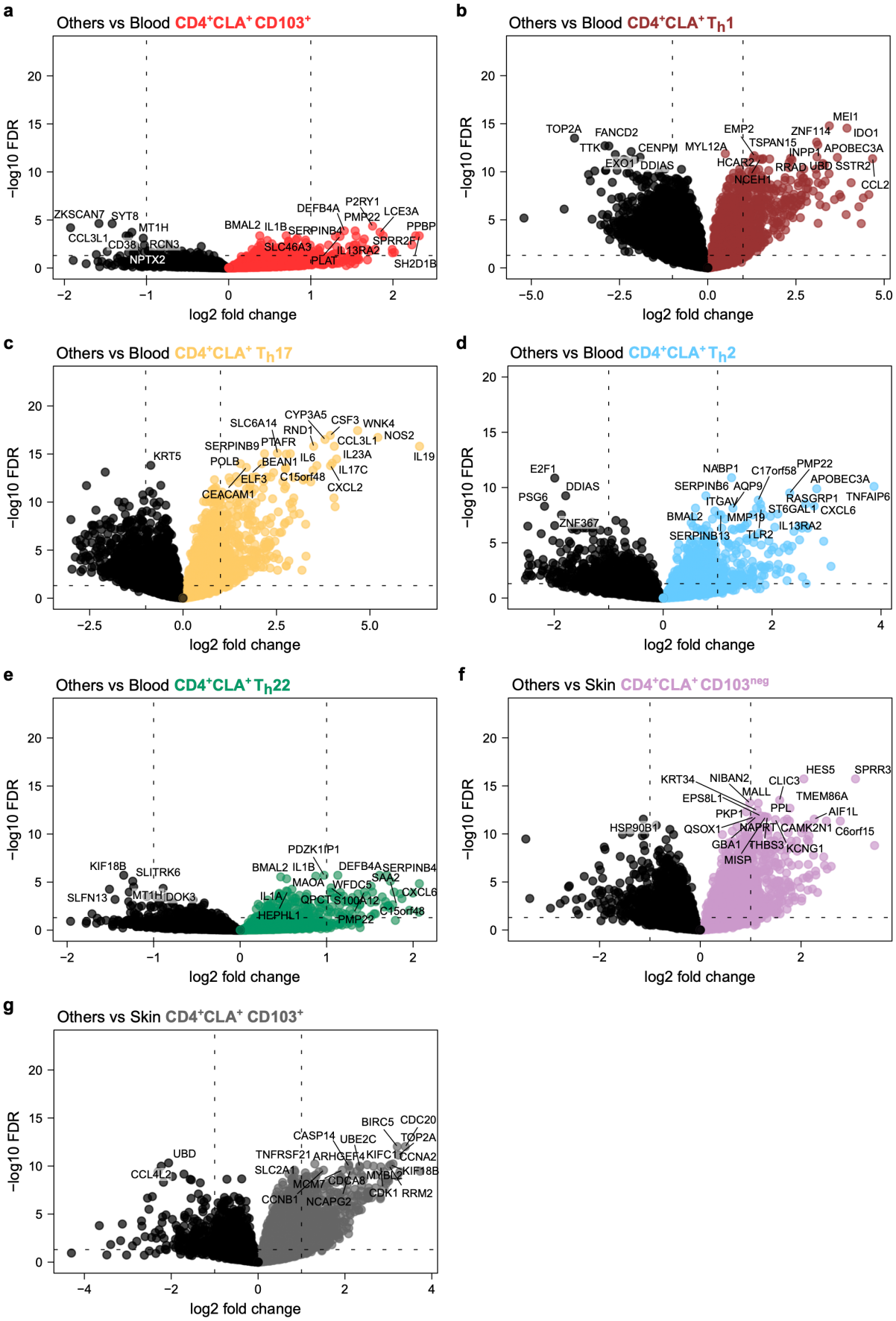

Supplementary Figure 2 (related to Figure 2). **CD4$^+$CLA$^+$ T cell-induced differential gene expression analysis of epithelial keratinocytes**. (**a-g**) Volcano plots showing differential gene expression analysis for KCs stimulated with each indicated CD4$^+$CLA$^+$ T$_h$ population. Cutoffs: log2 fold change >1 and -log10 FDR <0.05. The top 20 genes, ranked by FDR, are labeled on each plot.

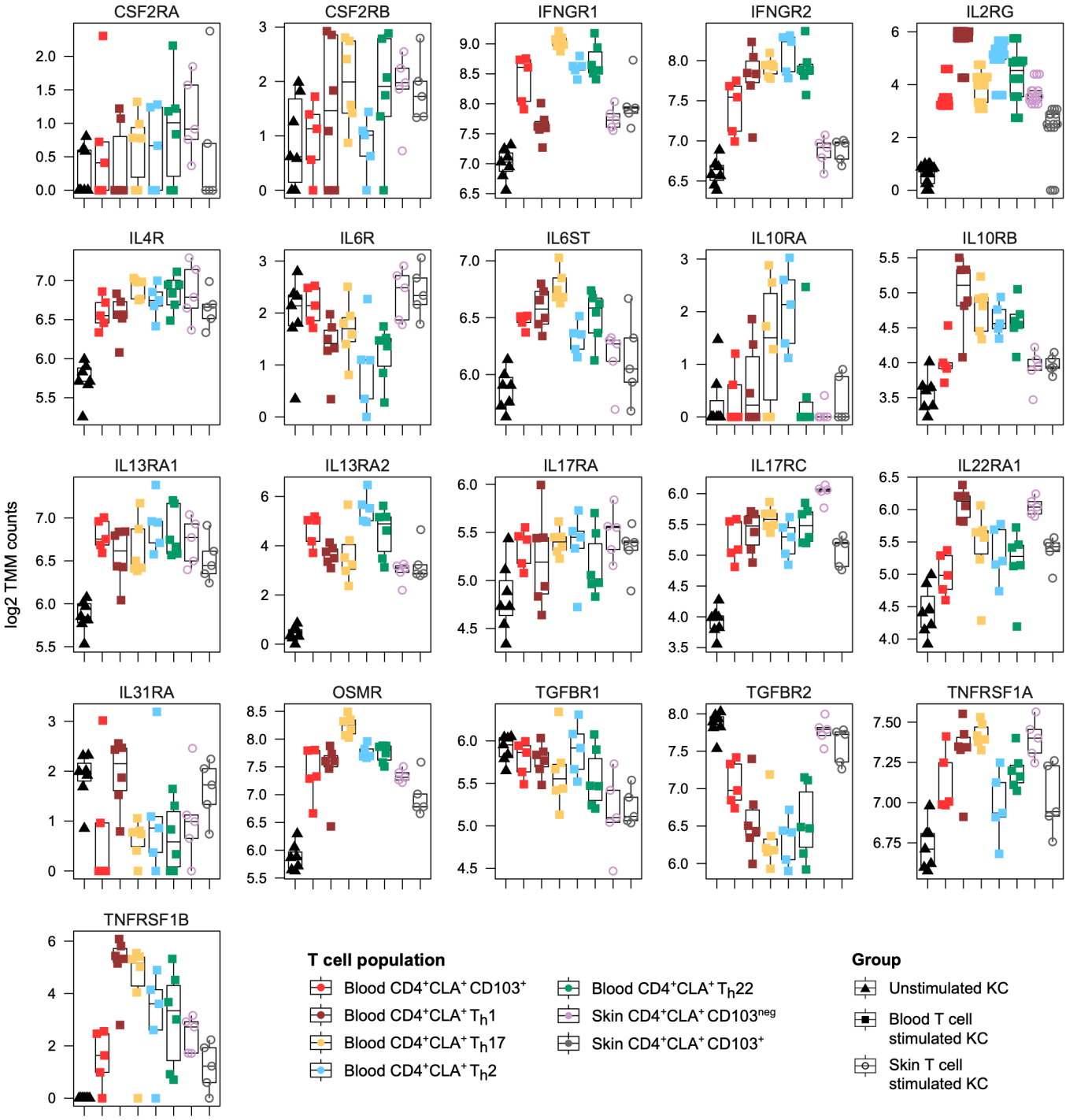

Supplementary Figure 3 (related to Figure 2). **Cytokine receptor gene expression changes induced by CD4$^+$CLA$^+$ T cells in epithelial keratinocytes**. Plots of log2 normalized expression counts using trimmed mean of M values (TMM) for each cytokine receptor gene in KCs stimulated with the indicated T cell populations (n=5-6 donors per population). Full statistical analysis of cytokine receptor gene expression is provided in **Supplementary Table 2**.

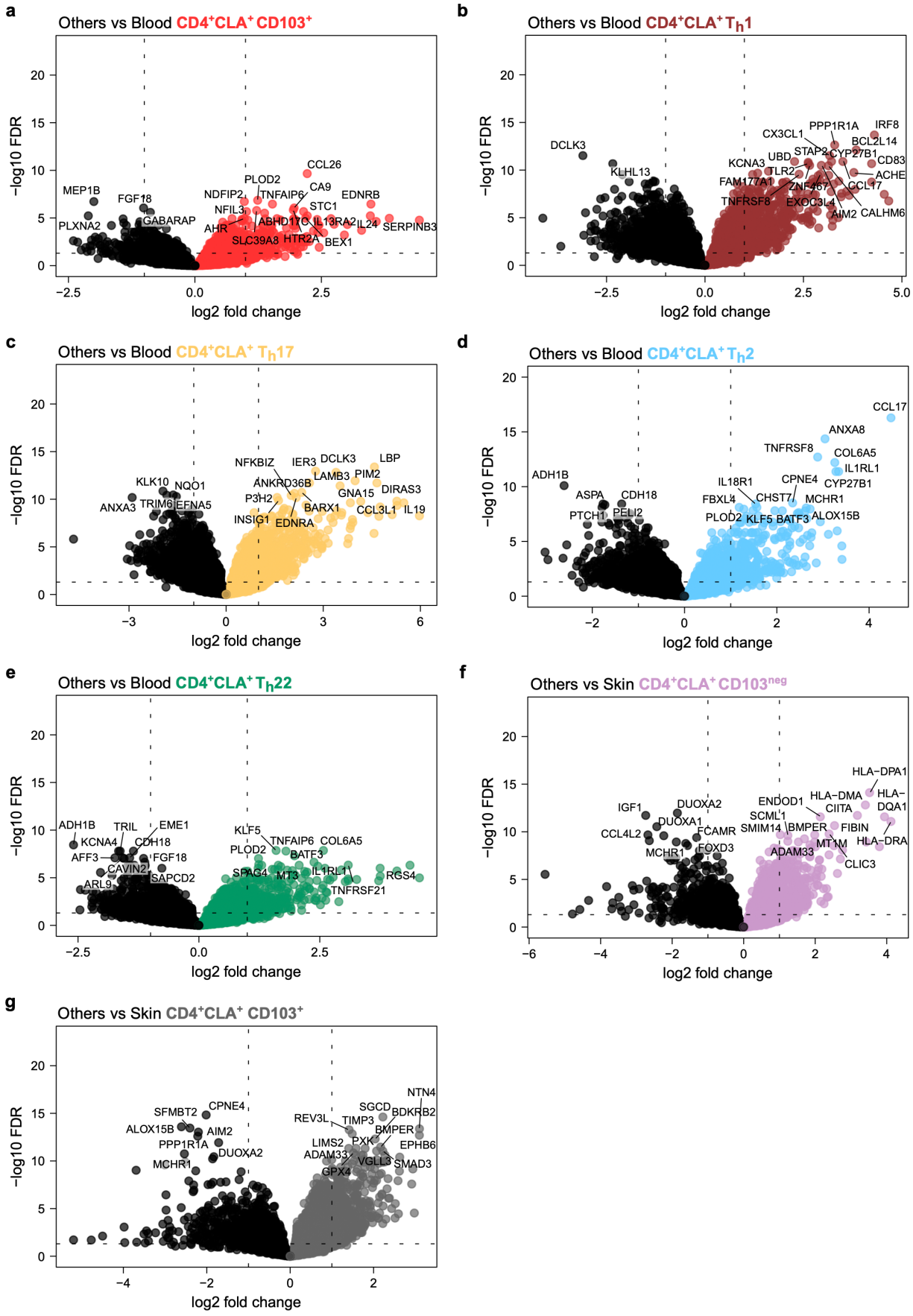

Supplementary Figure 4 (related to Figure 3). **CD4$^+$CLA$^+$ T cell-induced differential gene expression analysis of dermal fibroblasts**. (**a-g**) Volcano plots showing differential gene expression analysis for Fibs stimulated with each indicated CD4$^+$CLA$^+$ T$_h$ population. Cutoffs: log2 fold change >1 and -log10 FDR <0.05. The top 20 genes, ranked by FDR, are labeled on each plot.

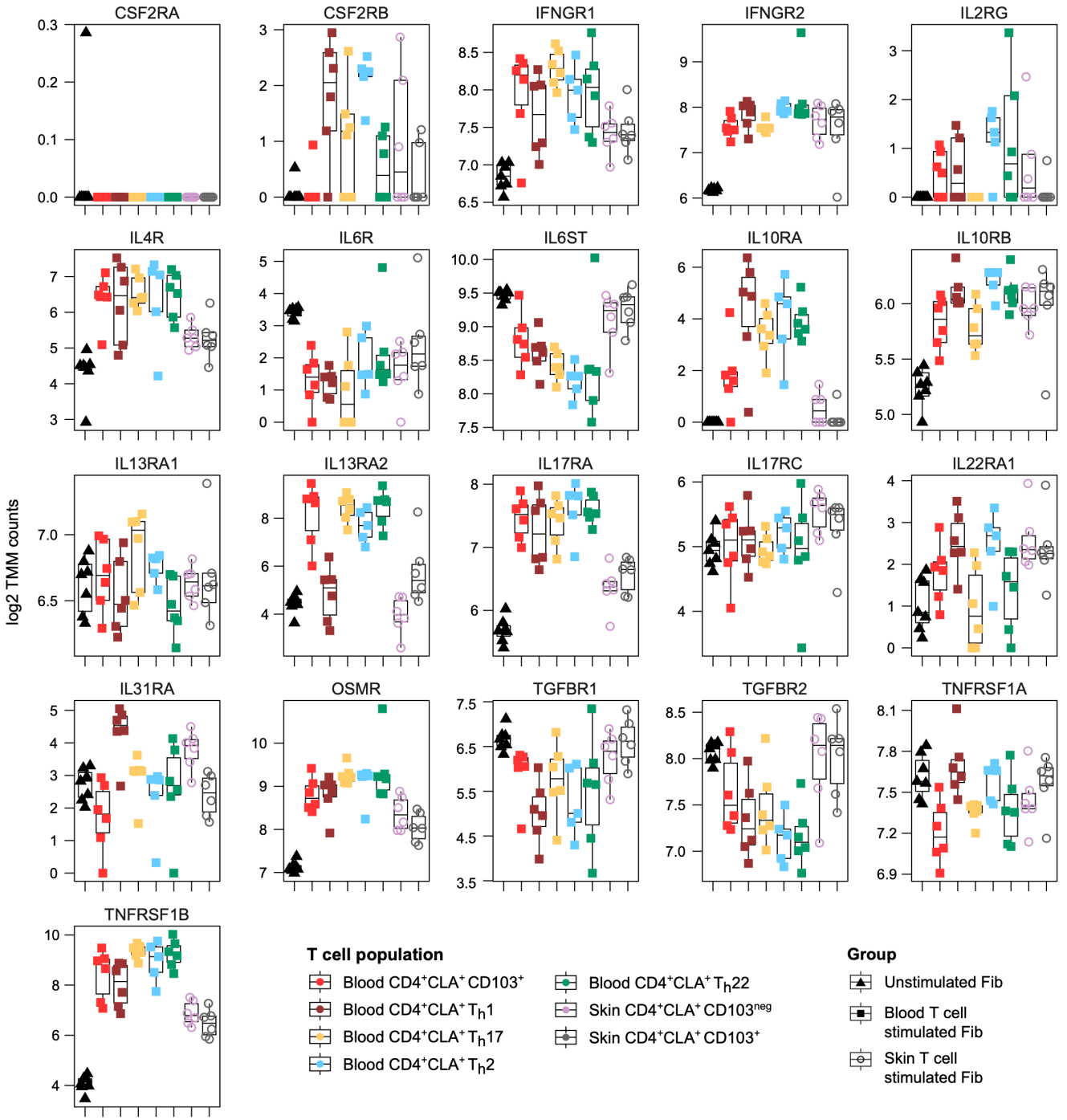

Supplementary Figure 5 (related to Figure 3). **Cytokine receptor gene expression changes induced by CD4$^+$CLA$^+$ T cells in epithelial keratinocytes**. Plots of log2 normalized expression counts using trimmed mean of M values (TMM) for each cytokine receptor gene in Fibs stimulated with the indicated T cell populations (n=5-6 donors per population). Full statistical analysis of cytokine receptor gene expression is provided in **Supplementary Table 3**.

a

	GSE137218	GSE166388	GSE31652
Samples (#)	84	8	30
Donors (#)	14	8	17
Disease group	Psoriasis	Psoriasis Control	Psoriasis
Treatment	Secukinumab	None	Ixekizumab
Tissue type	Lesional Non-Lesional	Lesional Healthy	Lesional
Visit (Days)	0, 4, 14, 42, 84	n/a	0, 14

b

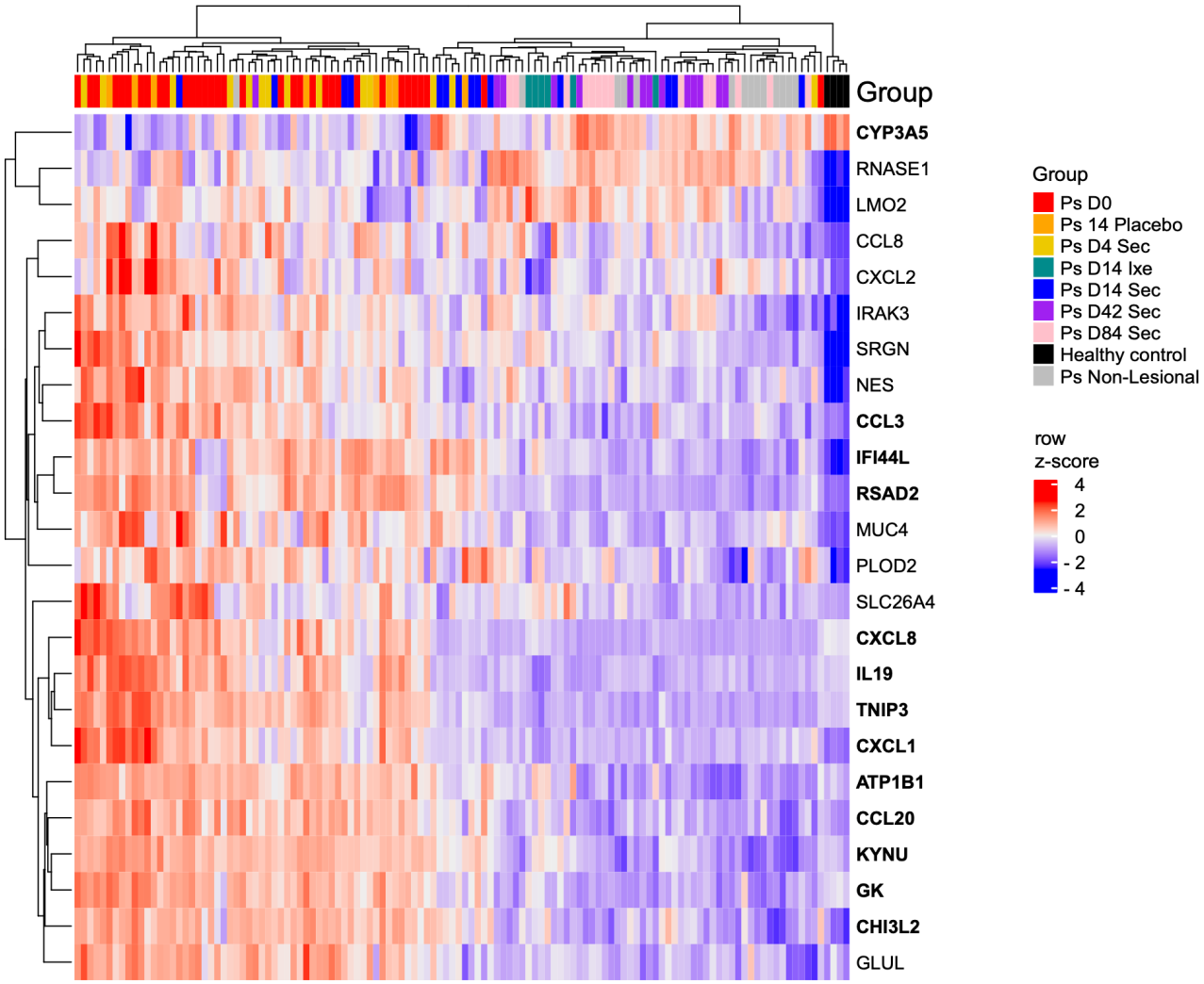

Supplementary Figure 6 (related to Figure 4). **CD4$^+$CLA$^+$ T$_h$17-dependent genes are altered in psoriasis patients undergoing anti-IL-17A therapy**. (**a**) Summary table showing cohort information for each of the three public Ps clinical trial data sets analyzed in Figure 4. (**b**) Heat map showing z-score expression changes of KC genes determined to be T$_h$17-dependent (Figure 2) within publicly available Ps patient data shown in Figure 4 for the indicated groups. Bolded genes are those that are significantly impacted by anti-IL-17A therapy compared with Ps Lesional D0. Full statistical analysis of T$_h$17-dependent gene expression is provided in **Supplementary Table 4**.

a

	GSE121212	GSE157194
Samples (#)	94	151
Donors (#)	44	57
Disease group	Control Atopic dermatitis	Atopic dermatitis
Treatment	None	Dupilumab
Tissue type	Healthy, Lesional Non-Lesional	Lesional Non-Lesional
Visit (Months)	n/a	0, 3

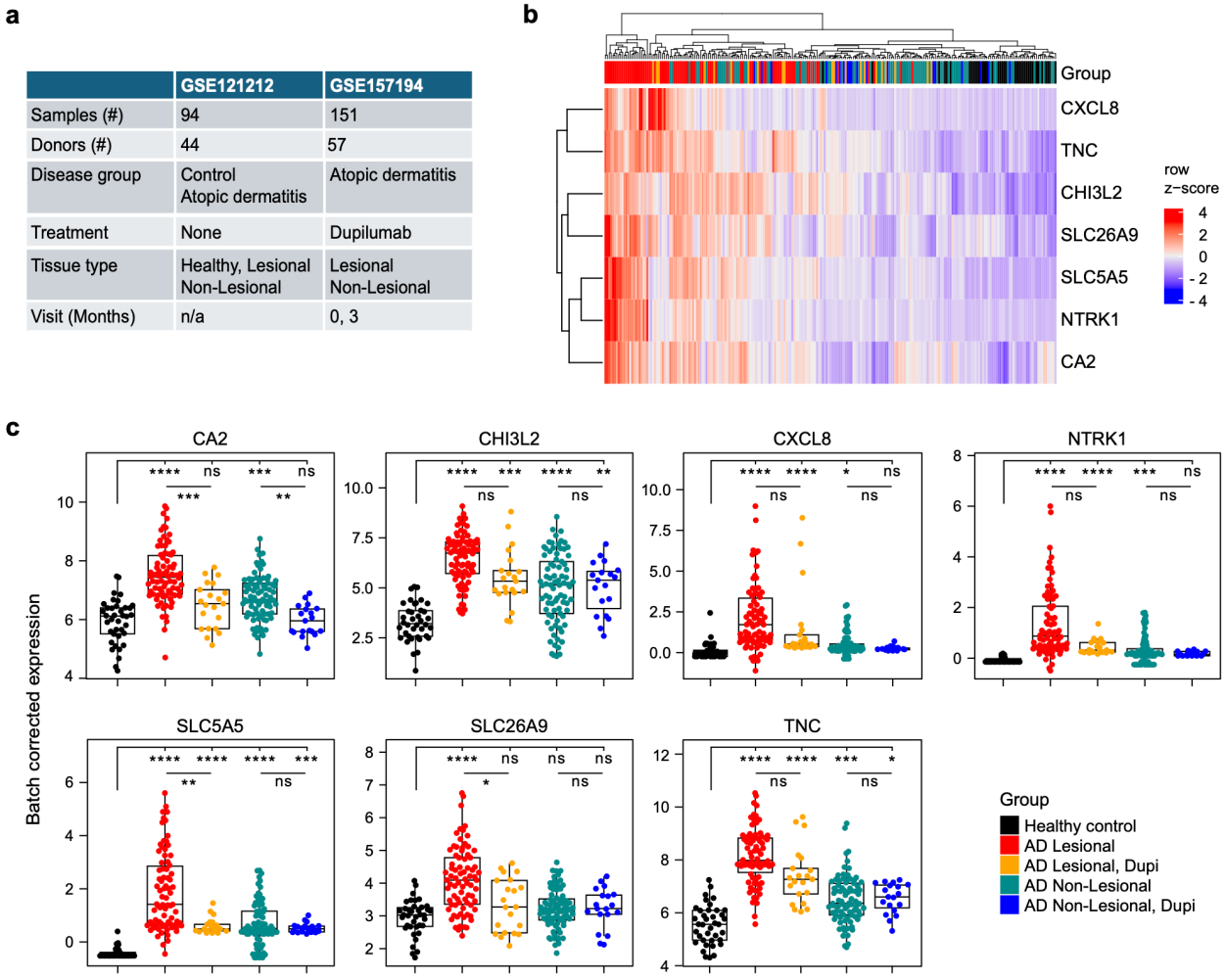

Supplementary Figure 7 (related to Figure 5). **CD4$^+$CLA$^+$ T$_h$2-dependent genes are altered in atopic dermatitis patients undergoing anti-IL-4Rα therapy**. (**a**) Summary table showing cohort information for the two public AD clinical trial data sets analyzed in Figure 5. (**b**) Heat map showing z-score expression changes of KC genes determined to be T$_h$2-dependent (Figure 2) within publicly available AD patient clinical data shown in Figure 5 for the indicated groups. (**c**) Individual gene plots for each T$_h$2-dependent KC gene identified within public AD clinical trial data sets. Error bars indicate mean ± SD; ns = not significant, *p ≤ 0.05, **p ≤ 0.01, ***p ≤ 0.001, and ****p ≤ 0.0001 (Student's *t*-test).

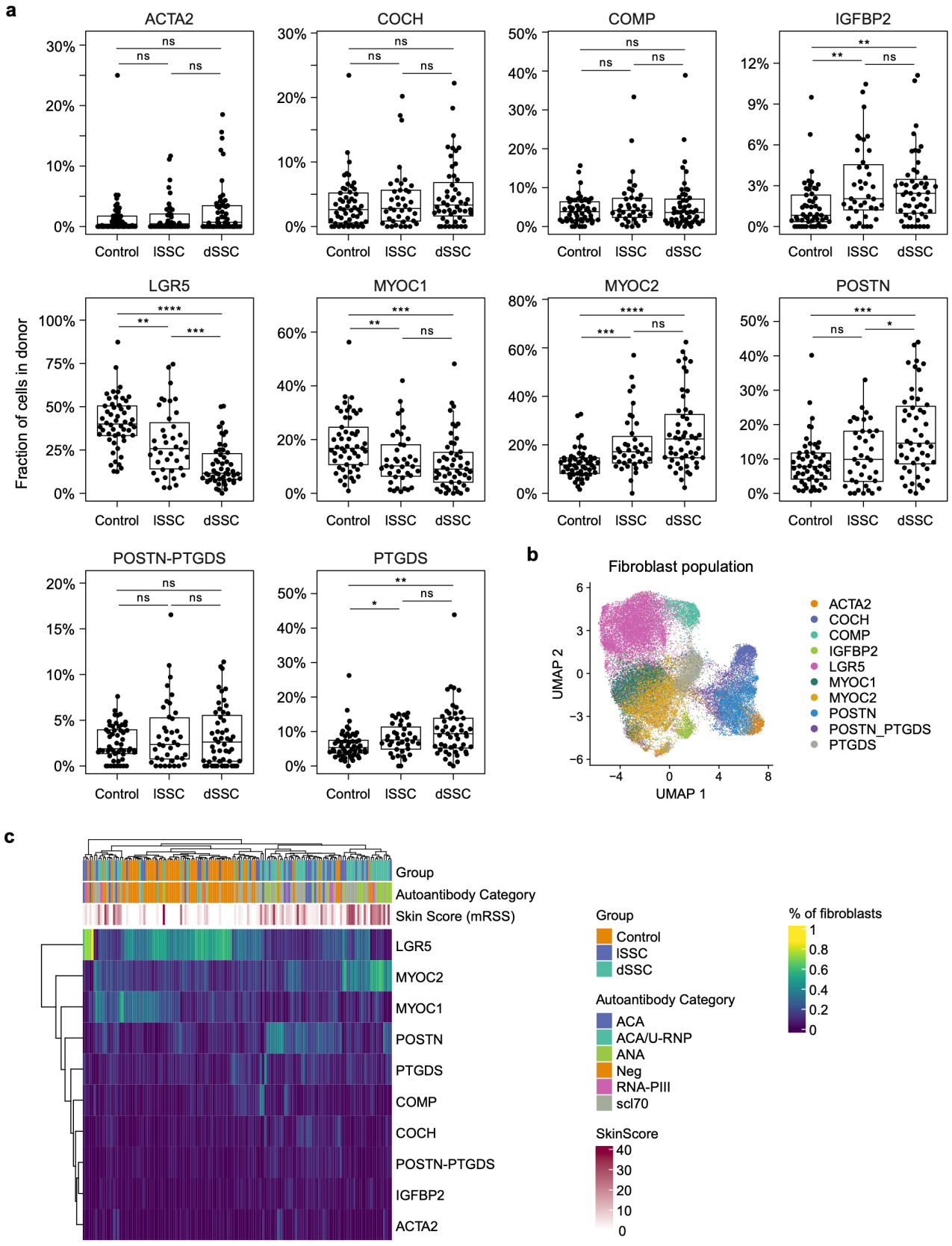

Supplementary Figure 8 (related to Figure 6). **Dermal fibroblast population analysis in healthy donors and scleroderma patients**. (**a**) Plots show the frequency of 10 previously described Fib subsets [GSE195452] as a percentage of total Fibs for each subject group. (**b**) Heat map shows the percentage of each Fib subset (*rows*) for each individual donor (*columns*). Group, Autoantibody Category, and scleroderma Skin Score (mRSS) is also shown for each donor. ACA, anti-centromere antibody; U-RNP, U1 small nuclear ribonucleoprotein particle; ANA, anti-nuclear antibody; Neg, auto-antibody negative; RNA-PIII, RNA polymerase III; scl70, scleroderma 70kDa/DNA-topoisomerase-1; mRSS, modified Rodnan skin score. Error bars indicate mean ± SD; ns = not significant, *p ≤ 0.05, **p ≤ 0.01, ***p ≤ 0.001, and ****p ≤ 0.0001 (Student's *t*-test).

References

1. Cheng JB, Sedgewick AJ, Finnegan AI, et al. Transcriptional Programming of Normal and Inflamed Human Epidermis at Single-Cell Resolution. *Cell Rep*. 2018;25(4):871-883. doi:10.1016/j.celrep.2018.09.006
2. Wang S, Drummond ML, Guerrero-Juarez CF, et al. Single cell transcriptomics of human epidermis identifies basal stem cell transition states. *Nat Commun*. 2020;11(1):4239. doi:10.1038/s41467-020-18075-7
3. Buechler MB, Pradhan RN, Krishnamurty AT, et al. Cross-tissue organization of the fibroblast lineage. *Nature*. 2021;593(7860):575-579. doi:10.1038/s41586-021-03549-5
4. Gur C, Wang SY, Sheban F, et al. LGR5 expressing skin fibroblasts define a major cellular hub perturbed in scleroderma. *Cell*. 2022;185(8):1373-1388.e20. doi:10.1016/j.cell.2022.03.011
5. Tabib T, Morse C, Wang T, Chen W, Lafyatis R. SFRP2/DPP4 and FMO1/LSP1 Define Major Fibroblast Populations in Human Skin. *J Invest Dermatol*. 2018;138(4):802-810. doi:10.1016/j.jid.2017.09.045
6. Tabib T, Huang M, Morse N, et al. Myofibroblast transcriptome indicates SFRP2hi fibroblast progenitors in systemic sclerosis skin. *Nat Commun*. 2021;12(1):4384. doi:10.1038/s41467-021-24607-6
7. Ho AW, Kupper TS. T cells and the skin: from protective immunity to inflammatory skin disorders. *Nat Rev Immunol*. 2019;19(8):490-502. doi:10.1038/s41577-019-0162-3
8. Sender R, Weiss Y, Navon Y, et al. The total mass, number, and distribution of immune cells in the human body. *Proc Natl Acad Sci U S A*. 2023;120(44):e2308511120. doi:10.1073/pnas.2308511120
9. Fuhlbrigge RC, Kieffer JD, Armerding D, Kupper TS. Cutaneous lymphocyte antigen is a specialized form of PSGL-1 expressed on skin-homing T cells. *Nature*. 1997;389(6654):978-981. doi:10.1038/40166
10. Clark RA, Chong B, Mirchandani N, et al. The vast majority of CLA+ T cells are resident in normal skin. *J Immunol*. 2006;176(7):4431-4439. doi:10.4049/jimmunol.176.7.4431
11. Duhen T, Duhen R, Lanzavecchia A, Sallusto F, Campbell DJ. Functionally distinct subsets of human FOXP3+ Treg cells that phenotypically mirror effector Th cells. *Blood*. 2012;119(19):4430-4440. doi:10.1182/blood-2011-11-392324
12. Klicznik MM, Morawski PA, Höllbacher B, et al. Human CD4+CD103+ cutaneous resident memory T cells are found in the circulation of healthy individuals. *Sci Immunol*. 2019;4(37):eaav8995. doi:10.1126/sciimmunol.aav8995
13. Kortekaas Krohn I, Aerts JL, Breckpot K, et al. T-cell subsets in the skin and their role in inflammatory skin disorders. *Allergy*. 2022;77(3):827-842. doi:10.1111/all.15104
14. Sabat R, Wolk K, Loyal L, Döcke WD, Ghoreschi K. T cell pathology in skin inflammation. *Semin Immunopathol*. 2019;41(3):359-377. doi:10.1007/s00281-019-00742-7
15. Duffin KC, Krueger GG. Genetic variations in cytokines and cytokine receptors associated with psoriasis found by genome-wide association. *J Invest Dermatol*. 2009;129(4):827-833. doi:10.1038/jid.2008.308
16. Stadler R, Mayer-da-Silva A, Bratzke B, Garbe C, Orfanos C. Interferons in dermatology. *J Am Acad Dermatol*. 1989;20(4):650-656. doi:10.1016/s0190-9622(89)70078-5
17. Chan TC, Hawkes JE, Krueger JG. Interleukin 23 in the skin: role in psoriasis pathogenesis and selective interleukin 23 blockade as treatment. *Ther Adv Chronic Dis*. 2018;9(5):111-119. doi:10.1177/2040622318759282
18. Silfvast-Kaiser A, Paek SY, Menter A. Anti-IL17 therapies for psoriasis. *Expert Opin Biol Ther*. 2019;19(1):45-54. doi:10.1080/14712598.2019.1555235
19. Song A, Lee SE, Kim JH. Immunopathology and Immunotherapy of Inflammatory Skin Diseases. *Immune Netw*. 2022;22(1):e7. doi:10.4110/in.2022.22.e7
20. Deckers J, Anbergen T, Hokke AM, et al. Engineering cytokine therapeutics. *Nat Rev Bioeng*. 2023;1(4):286-303. doi:10.1038/s44222-023-00030-y
21. Höllbacher B, Duhen T, Motley S, Klicznik MM, Gratz IK, Campbell DJ. Transcriptomic Profiling of Human Effector and Regulatory T Cell Subsets Identifies Predictive Population Signatures. *Immunohorizons*. 2020;4(10):585-596. doi:10.4049/immunohorizons.2000037
22. de Jesús-Gil C, Sans-de SanNicolàs L, García-Jiménez I, et al. The Translational Relevance of Human Circulating Memory Cutaneous Lymphocyte-Associated Antigen Positive T Cells in Inflammatory Skin Disorders. *Front Immunol*. 2021;12:652613. doi:10.3389/fimmu.2021.652613
23. Kominsky DJ, Campbell EL, Ehrentraut SF, et al. IFN-γ-mediated induction of an apical IL-10 receptor on polarized intestinal epithelia. *J Immunol*. 2014;192(3):1267-1276. doi:10.4049/jimmunol.1301757

24. Jenkins W, Perone P, Walker K, et al. Fibroblast response to lanthanoid metal ion stimulation: potential contribution to fibrotic tissue injury. *Biol Trace Elem Res*. 2011;144(1-3):621-635. doi:10.1007/s12011-011-9041-x
25. Fichtner-Feigl S, Strober W, Kawakami K, Puri RK, Kitani A. IL-13 signaling through the IL-13alpha2 receptor is involved in induction of TGF-beta1 production and fibrosis. *Nat Med*. 2006;12(1):99-106. doi:10.1038/nm1332
26. Chao H, Zheng L, Hsu P, et al. IL-13RA2 downregulation in fibroblasts promotes keloid fibrosis via JAK/STAT6 activation. *JCI Insight*. 2023;8(6):e157091. doi:10.1172/jci.insight.157091
27. Dillon SR, Sprecher C, Hammond A, et al. Interleukin 31, a cytokine produced by activated T cells, induces dermatitis in mice. *Nat Immunol*. 2004;5(7):752-760. doi:10.1038/ni1084
28. Bilsborough J, Leung DYM, Maurer M, et al. IL-31 is associated with cutaneous lymphocyte antigen-positive skin homing T cells in patients with atopic dermatitis. *J Allergy Clin Immunol*. 2006;117(2):418-425. doi:10.1016/j.jaci.2005.10.046
29. Vu TT, Koguchi-Yoshioka H, Watanabe R. Skin-Resident Memory T Cells: Pathogenesis and Implication for the Treatment of Psoriasis. *J Clin Med*. 2021;10(17):3822. doi:10.3390/jcm10173822
30. Esaki H, Brunner PM, Renert-Yuval Y, et al. Early-onset pediatric atopic dermatitis is TH2 but also TH17 polarized in skin. *J Allergy Clin Immunol*. 2016;138(6):1639-1651. doi:10.1016/j.jaci.2016.07.013
31. Tsoi LC, Rodriguez E, Degenhardt F, et al. Atopic Dermatitis Is an IL-13-Dominant Disease with Greater Molecular Heterogeneity Compared to Psoriasis. *J Invest Dermatol*. 2019;139(7):1480-1489. doi:10.1016/j.jid.2018.12.018
32. Gittler JK, Shemer A, Suárez-Fariñas M, et al. Progressive activation of T(H)2/T(H)22 cytokines and selective epidermal proteins characterizes acute and chronic atopic dermatitis. *J Allergy Clin Immunol*. 2012;130(6):1344-1354. doi:10.1016/j.jaci.2012.07.012
33. Aboobacker S, Kurn H, Al Aboud AM. Secukinumab. In: *StatPearls*. StatPearls Publishing; 2024. Accessed July 26, 2024. http://www.ncbi.nlm.nih.gov/books/NBK537091/
34. Preuss CV, Quick J. Ixekizumab. In: *StatPearls*. StatPearls Publishing; 2024. Accessed July 26, 2024. http://www.ncbi.nlm.nih.gov/books/NBK431088/
35. Gade A, Ghani H, Patel P, Rubenstein R. Dupilumab. In: *StatPearls*. StatPearls Publishing; 2024. Accessed July 26, 2024. http://www.ncbi.nlm.nih.gov/books/NBK585114/
36. Guttman-Yassky E, Kabashima K, Staumont-Salle D, et al. Targeting IL-13 with tralokinumab normalizes type 2 inflammation in atopic dermatitis both early and at 2 years. *Allergy*. 2024;79(6):1560-1572. doi:10.1111/all.16108
37. Ganier C, Mazin P, Herrera-Oropeza G, et al. Multiscale spatial mapping of cell populations across anatomical sites in healthy human skin and basal cell carcinoma. *Proc Natl Acad Sci U S A*. 2024;121(2):e2313326120. doi:10.1073/pnas.2313326120
38. Bertelsen T, Ljungberg C, Litman T, et al. IκBζ is a key player in the antipsoriatic effects of secukinumab. *J Allergy Clin Immunol*. 2020;145(1):379-390. doi:10.1016/j.jaci.2019.09.029
39. Qiu X, Zheng L, Liu X, et al. ULK1 Inhibition as a Targeted Therapeutic Strategy for Psoriasis by Regulating Keratinocytes and Their Crosstalk With Neutrophils. *Front Immunol*. 2021;12:714274. doi:10.3389/fimmu.2021.714274
40. Krueger JG, Fretzin S, Suárez-Fariñas M, et al. IL-17A is essential for cell activation and inflammatory gene circuits in subjects with psoriasis. *J Allergy Clin Immunol*. 2012;130(1):145-154.e9. doi:10.1016/j.jaci.2012.04.024
41. Herrera-Acosta E, Garriga-Martina GG, Suárez-Pérez JA, Martínez-García EA, Herrera-Ceballos E. Comparative study of the efficacy and safety of secukinumab vs ixekizumab in moderate-to-severe psoriasis after 1 year of treatment: Real-world practice. *Dermatol Ther*. 2020;33(3):e13313. doi:10.1111/dth.13313
42. Ellinghaus D, Jostins L, Spain SL, et al. Analysis of five chronic inflammatory diseases identifies 27 new associations and highlights disease-specific patterns at shared loci. *Nat Genet*. 2016;48(5):510-518. doi:10.1038/ng.3528
43. Folkersen L, Gustafsson S, Wang Q, et al. Genomic and drug target evaluation of 90 cardiovascular proteins in 30,931 individuals. *Nat Metab*. 2020;2(10):1135-1148. doi:10.1038/s42255-020-00287-2
44. Dimas AS, Deutsch S, Stranger BE, et al. Common regulatory variation impacts gene expression in a cell type-dependent manner. *Science*. 2009;325(5945):1246-1250. doi:10.1126/science.1174148
45. Quach H, Rotival M, Pothlichet J, et al. Genetic Adaptation and Neandertal Admixture Shaped the Immune System of Human Populations. *Cell*. 2016;167(3):643-656.e17. doi:10.1016/j.cell.2016.09.024

46. Liu JZ, van Sommeren S, Huang H, et al. Association analyses identify 38 susceptibility loci for inflammatory bowel disease and highlight shared genetic risk across populations. *Nat Genet*. 2015;47(9):979-986. doi:10.1038/ng.3359
47. Li YR, Li J, Zhao SD, et al. Meta-analysis of shared genetic architecture across ten pediatric autoimmune diseases. *Nat Med*. 2015;21(9):1018-1027. doi:10.1038/nm.3933
48. Javierre BM, Burren OS, Wilder SP, et al. Lineage-Specific Genome Architecture Links Enhancers and Non-coding Disease Variants to Target Gene Promoters. *Cell*. 2016;167(5):1369-1384.e19. doi:10.1016/j.cell.2016.09.037
49. Furue K, Ito T, Tsuji G, Nakahara T, Furue M. The CCL20 and CCR6 axis in psoriasis. *Scand J Immunol*. 2020;91(3):e12846. doi:10.1111/sji.12846
50. Witte E, Kokolakis G, Witte K, et al. IL-19 is a component of the pathogenetic IL-23/IL-17 cascade in psoriasis. *J Invest Dermatol*. 2014;134(11):2757-2767. doi:10.1038/jid.2014.308
51. Furue M, Furue K, Tsuji G, Nakahara T. Interleukin-17A and Keratinocytes in Psoriasis. *Int J Mol Sci*. 2020;21(4):1275. doi:10.3390/ijms21041275
52. Watarai A, Amoh Y, Maejima H, Hamada Y, Katsuoka K. Nestin expression is increased in the suprabasal epidermal layer in psoriasis vulgaris. *Acta Derm Venereol*. 2013;93(1):39-43. doi:10.2340/00015555-1420
53. Möbus L, Rodriguez E, Harder I, et al. Atopic dermatitis displays stable and dynamic skin transcriptome signatures. *J Allergy Clin Immunol*. 2021;147(1):213-223. doi:10.1016/j.jaci.2020.06.012
54. Tsoi LC, Rodriguez E, Stölzl D, et al. Progression of acute-to-chronic atopic dermatitis is associated with quantitative rather than qualitative changes in cytokine responses. *J Allergy Clin Immunol*. 2020;145(5):1406-1415. doi:10.1016/j.jaci.2019.11.047
55. Kamsteeg M, Jansen P a. M, van Vlijmen-Willems IMJJ, et al. Molecular diagnostics of psoriasis, atopic dermatitis, allergic contact dermatitis and irritant contact dermatitis. *Br J Dermatol*. 2010;162(3):568-578. doi:10.1111/j.1365-2133.2009.09547.x
56. Kamsteeg M, Bergers M, de Boer R, et al. Type 2 helper T-cell cytokines induce morphologic and molecular characteristics of atopic dermatitis in human skin equivalent. *Am J Pathol*. 2011;178(5):2091-2099. doi:10.1016/j.ajpath.2011.01.037
57. Wynn TA, Ramalingam TR. Mechanisms of fibrosis: therapeutic translation for fibrotic disease. *Nat Med*. 2012;18(7):1028-1040. doi:10.1038/nm.2807
58. Fang D, Chen B, Lescoat A, Khanna D, Mu R. Immune cell dysregulation as a mediator of fibrosis in systemic sclerosis. *Nat Rev Rheumatol*. 2022;18(12):683-693. doi:10.1038/s41584-022-00864-7
59. Gabrielli A, Avvedimento EV, Krieg T. Scleroderma. *N Engl J Med*. 2009;360(19):1989-2003. doi:10.1056/NEJMra0806188
60. Mulcaire-Jones E, Low AHL, Domsic R, Whitfield ML, Khanna D. Advances in biological and targeted therapies for systemic sclerosis. *Expert Opinion on Biological Therapy*. 2023;23(4):325-339. doi:10.1080/14712598.2023.2196009
61. Bragulla HH, Homberger DG. Structure and functions of keratin proteins in simple, stratified, keratinized and cornified epithelia. *J Anat*. 2009;214(4):516-559. doi:10.1111/j.1469-7580.2009.01066.x
62. Wang J, Wang C, Liu L, et al. Adverse events associated with anti-IL-17 agents for psoriasis and psoriatic arthritis: a systematic scoping review. *Front Immunol*. 2023;14:993057. doi:10.3389/fimmu.2023.993057
63. Bieber T. Interleukin-13: Targeting an underestimated cytokine in atopic dermatitis. *Allergy*. 2020;75(1):54-62. doi:10.1111/all.13954
64. Gordon KB, Blauvelt A, Papp KA, et al. Phase 3 Trials of Ixekizumab in Moderate-to-Severe Plaque Psoriasis. *N Engl J Med*. 2016;375(4):345-356. doi:10.1056/NEJMoa1512711
65. Damiani G, Conic RRZ, de Vita V, et al. When IL-17 inhibitors fail: Real-life evidence to switch from secukinumab to adalimumab or ustekinumab. *Dermatol Ther*. 2019;32(2):e12793. doi:10.1111/dth.12793
66. Megna M, Ruggiero A, Martora F, Vallone Y, Guerrasio G, Potestio L. Long-Term Efficacy and Safety of Guselkumab in Psoriasis Patients Who Failed Anti-IL17: A Two-Year Real-Life Study. *J Clin Med*. 2024;13(9):2691. doi:10.3390/jcm13092691
67. Simpson EL, Bieber T, Guttman-Yassky E, et al. Two Phase 3 Trials of Dupilumab versus Placebo in Atopic Dermatitis. *N Engl J Med*. 2016;375(24):2335-2348. doi:10.1056/NEJMoa1610020

68. Wu NL, Huang DY, Tsou HN, Lin YC, Lin WW. Syk mediates IL-17-induced CCL20 expression by targeting Act1-dependent K63-linked ubiquitination of TRAF6. *J Invest Dermatol*. 2015;135(2):490-498. doi:10.1038/jid.2014.383
69. Woodward Davis AS, Roozen HN, Dufort MJ, et al. The human tissue-resident CCR5+ T cell compartment maintains protective and functional properties during inflammation. *Sci Transl Med*. 2019;11(521):eaaw8718. doi:10.1126/scitranslmed.aaw8718
70. Sgambelluri F, Diani M, Altomare A, et al. A role for CCR5(+)CD4 T cells in cutaneous psoriasis and for CD103(+) CCR4(+) CD8 Teff cells in the associated systemic inflammation. *J Autoimmun*. 2016;70:80-90. doi:10.1016/j.jaut.2016.03.019
71. Reich K, Armstrong AW, Langley RG, et al. Guselkumab versus secukinumab for the treatment of moderate-to-severe psoriasis (ECLIPSE): results from a phase 3, randomised controlled trial. *Lancet*. 2019;394(10201):831-839. doi:10.1016/S0140-6736(19)31773-8
72. Kamsteeg M, Zeeuwen PLJM, de Jongh GJ, et al. Increased expression of carbonic anhydrase II (CA II) in lesional skin of atopic dermatitis: regulation by Th2 cytokines. *J Invest Dermatol*. 2007;127(7):1786-1789. doi:10.1038/sj.jid.5700752
73. Rochman M, Kartashov AV, Caldwell JM, et al. Neurotrophic tyrosine kinase receptor 1 is a direct transcriptional and epigenetic target of IL-13 involved in allergic inflammation. *Mucosal Immunol*. 2015;8(4):785-798. doi:10.1038/mi.2014.109
74. Ogawa K, Ito M, Takeuchi K, et al. Tenascin-C is upregulated in the skin lesions of patients with atopic dermatitis. *J Dermatol Sci*. 2005;40(1):35-41. doi:10.1016/j.jdermsci.2005.06.001
75. Peng S, Chen M, Yin M, Feng H. Identifying the Potential Therapeutic Targets for Atopic Dermatitis Through the Immune Infiltration Analysis and Construction of a ceRNA Network. *CCID*. 2021;Volume 14:437-453. doi:10.2147/CCID.S310426
76. Simpson EL, Schlievert PM, Yoshida T, et al. Rapid reduction in Staphylococcus aureus in atopic dermatitis subjects following dupilumab treatment. *J Allergy Clin Immunol*. 2023;152(5):1179-1195. doi:10.1016/j.jaci.2023.05.026
77. Zhu H, Luo H, Skaug B, et al. Fibroblast Subpopulations in Systemic Sclerosis: Functional Implications of Individual Subpopulations and Correlations with Clinical Features. *J Invest Dermatol*. 2024;144(6):1251-1261.e13. doi:10.1016/j.jid.2023.09.288
78. Ho KT, Reveille JD. The clinical relevance of autoantibodies in scleroderma. *Arthritis Res Ther*. 2003;5(2):80-93. doi:10.1186/ar628
79. Werner G, Sanyal A, Mirizio E, et al. Single-Cell Transcriptome Analysis Identifies Subclusters with Inflammatory Fibroblast Responses in Localized Scleroderma. *Int J Mol Sci*. 2023;24(12):9796. doi:10.3390/ijms24129796
80. Ritchie ME, Phipson B, Wu D, et al. limma powers differential expression analyses for RNA-sequencing and microarray studies. *Nucleic Acids Res*. 2015;43(7):e47. doi:10.1093/nar/gkv007
81. Leek JT, Johnson WE, Parker HS, Jaffe AE, Storey JD. The sva package for removing batch effects and other unwanted variation in high-throughput experiments. *Bioinformatics*. 2012;28(6):882-883. doi:10.1093/bioinformatics/bts034
82. Chen EY, Tan CM, Kou Y, et al. Enrichr: interactive and collaborative HTML5 gene list enrichment analysis tool. *BMC Bioinformatics*. 2013;14:128. doi:10.1186/1471-2105-14-128
83. Milacic M, Beavers D, Conley P, et al. The Reactome Pathway Knowledgebase 2024. *Nucleic Acids Res*. 2024;52(D1):D672-D678. doi:10.1093/nar/gkad1025
84. Sollis E, Mosaku A, Abid A, et al. The NHGRI-EBI GWAS Catalog: knowledgebase and deposition resource. *Nucleic Acids Res*. 2023;51(D1):D977-D985. doi:10.1093/nar/gkac1010
85. Hao Y, Hao S, Andersen-Nissen E, et al. Integrated analysis of multimodal single-cell data. *Cell*. 2021;184(13):3573-3587.e29. doi:10.1016/j.cell.2021.04.048